Monte Carlo Computations of Neoclassical Transport

W. Lotz and J. Nührenberg

IPP 0/49

December 1987

MAX-PLANCK-INSTITUT FÜR PLASMAPHYSIK

8046 GARCHING BEI MÜNCHEN

MAX-PLANCK-INSTITUT FÜR PLASMAPHYSIK

GARCHING BEI MÜNCHEN

Monte Carlo Computations of Neoclassical Transport

W. LOTZ AND J. NÜHRENBERG

IPP 0/49 December 1987

Die nachstehende Arbeit wurde im Rahmen des Vertrages zwischen dem Max-Planck-Institut für Plasmaphysik und der Europäischen Atomgemeinschaft über die Zusammenarbeit auf dem Gebiete der Plasmaphysik durchgeführt.

IPP 0/49 December 1987

Monte Carlo Computations of Neoclassical Transport

W. LOTZ AND J. NÜHRENBERG

Abstract

Neoclassical transport coefficients and confinement times in stellarators of general geometry and tokamaks with and without ripple are computed by Monte Carlo simulation over wide ranges of mean free paths, ratios of plasma to gyro radius, and radial electric fields.

The results for monoenergetic particles can be represented by simple formulas using a transport coefficient normalized to the tokamak plateau value and a mean free path normalized to half the connection length.

Transport coefficients obtained with monoenergetic particles subjected to pitch angle scattering and energy relaxation are convoluted with a Maxwellian energy distribution. The results are compared with theory and with simulations using a particle distribution subjected to pitch angle as well as energy scattering. The overall agreement is good.

Transport coefficients with Maxwellian energy distributions for $\ell = 2$ stellarators and for various other stellarator configurations are shown. Particle transport as well as energy transport coefficients for these configurations are computed for ions (deuterons) as well as for electrons. Estimates of particle and energy confinement times are also obtained.

I. INTRODUCTION

Monte Carlo methods previously developed[1–7] for calculating neoclassical transport coefficients and confinement times in stellarators and tokamaks with or without ripple can be used not only for monoenergetic particles, but also for particles which have an energy distribution.

It turns out that the computing time needed for a Monto Carlo simulation including pitch angle and energy scattering is an order of magnitude larger than that needed for a "monoenergetic" simulation without energy scattering. It would therefore be of advantage to derive the results for a Maxwellian energy distribution by convoluting the results of a monoenergetic particle distribution not only for the case without electric field but also for the case with non-zero radial electric field.

It is found that this procedure indeed gives correct results.

This paper is organized as follows: Section II introduces the relevant notations. In Sec. III formulas are given for local transport coefficients with electric field. The limit of vanishing electric field and very long mean free path has to be treated by a non-local loss rate calculation which is described in Sec. IV. Sec. V gives the convolution with a Maxwellian energy distribution and the full Monte Carlo simulation. Sec. VI is concerned with particle and energy fluxes and confinement times. Sec. VII describes applications to W VII-AS,[8] Helias49,[9] TJ-II,[10] ATF,[11] and Heliotron-E[12] configurations. Sec. VIII presents some conclusions.

II. LOCAL TRANSPORT COEFFICIENTS WITHOUT ELECTRIC FIELD

If the value Q_ϱ of the ratio of plasma radius a to gyro radius ϱ of the particles is sufficiently large, a local transport coefficient can be calculated with the help of Boozer's Monte Carlo equivalent of the pitch angle scattering operator. The results for monoenergetic particles can be presented in a normalized way[3] and are briefly repeated here for convenience. A normalized mean free path L^* is used:

$$L^* = \Lambda / L_c, \qquad L_c = \pi R_o / \iota, \tag{1}$$

where Λ is the mean free path, L_c half the connection length, R_o the major torus radius, and ι the rotational transform (or twist) on the magnetic surface considered. A normalized transport coefficient D^* is introduced by

$$D^* = D / D_P, \tag{2}$$

where D_P is the plateau value

$$D_P = 0.64 \, \frac{\varrho^2 \, v}{\iota^2 \, L_c} = 0.64 \, \frac{\varrho^2 \, v}{\iota \, \pi R_o} \, , \tag{3}$$

$v = (2E/m)^{1/2}$ being the particle velocity and $\varrho = mv/eB_o$ the formal gyro radius, where B_o is the main magnetic field at R_o.

With these normalizations the Pfirsch-Schlüter regime, the tokamak banana regime, and the ripple regime are given, respectively, by

$$D^*_{PS} = C_{PS}/L^*, \qquad D^*_B = C_B \, A^{3/2}/L^*, \qquad D^*_R = 1.65 \, C_R \, \delta_e^{3/2} L^*, \tag{4}$$

where $A = R_o/r$ is the aspect ratio of the magnetic surface considered, and δ_e is the effective ripple. The coefficients C_{PS}, C_B, and C_R are near 1.0 for a (rippled) tokamak, but may be different for a stellarator.

Fig. 1 gives the results without electric field for an $\ell = 2$ stellararor and a tokamak with and without ripple, the three cases being chosen in such a way that they have the same aspect ratio and rotational transform and, as far as the stellarator and rippled tokamak are concerned, the same effective ripple.

III. LOCAL TRANSPORT COEFFICIENTS WITH ELECTRIC FIELD

Figures 2 and 3 give results for an $\ell = 2$ stellarator for various values of Q_ϱ and the electric field F in the case of monoenergetic particles.

F is related to the potential $\phi = \phi_o(1-\psi)$ by $F = +\phi_o 2r/a^2$ ($\phi_o > 0$ is repulsive to positive ions), where r is the formal radius of the magnetic surface with normalized flux ψ.

As has been shown earlier,[5,6] the $\sqrt{\nu}$ regime and the ν regime can generally be represented by

$$\begin{aligned} D^*_{\nu^{1/2}} &= C_{\nu^{1/2}}\, H^{1.5}\, \sqrt{\nu^*}\,, \\ D^*_{\nu} &= C_{\nu}\, H^2\, \nu^*\,, \\ H &= \frac{2}{A}\frac{\iota}{\varrho}\frac{E}{eF} = \frac{\iota a Q_\varrho}{R_o}\frac{E}{e\phi_o}\,, \end{aligned} \tag{5}$$

where E is the kinetic particle energy and $\nu^* = 1/L^*$.

The coefficients $C_{\nu^{1/2}}$ and C_ν are of order 0.1 and 1 respectively.

The domain of validity of Eq. (5) is restricted by two limiting cases. For very weak electric field ($H \to \infty$) the concept of a local transport coefficient is not valid, so that a critical value H_c of H has to be used, $H \le H_c$. This value is determined from a non-local loss rate calculation (see next section). For strong electric field ($H \to 1$), the transport coefficient does not fall below tokamak banana transport, so that a smooth transition to this transport regime has to be effected.

Analysis of the computational results shows that close modelling is obtained with the following formulas:

$\sqrt{\nu}$ regime:

$$C_{\nu^{1/2}} = C_{11}\,\frac{1 + C_{12}\frac{A}{H^{3/2}}}{1 + \left(\frac{H}{H_c}\right)^{3/2}}, \tag{6}$$

ν regime:

$$C_{\nu} = C_{21}\,\frac{1 + C_{22}\frac{A^{3/2}}{H^2}}{1 + \left(\frac{H}{H_c}\right)^{2}}, \tag{7}$$

at aspect ratio $A = R_o/r$, $H_c = 0.53\ \iota\, Q_\varrho$, and $H > 1$.

From figures like Figs. 2 to 6 the constants C_{ik} can be derived and are given in Table I.

Note that the detailed ripple structure enters only relatively weakly through the coefficients C_{ik}. This is in accordance with the fact that the limiting cases depend only weakly on the ripple structure.

IV. LOSS RATES WITHOUT ELECTRIC FIELD

Loss rates for monoenergetic particles can be represented as well in a normalized way[5,6]:

$$S^* = S/S_P, \tag{8}$$

with the plateau value

$$S_P = 3.6\ \frac{v}{Q_\ell^2\ \iota\ \pi R_o} = 5.7 \frac{D_P}{a^2} = \left(\frac{2.4}{a}\right)^2 D_P\ . \tag{9}$$

With this normalization the Pfirsch-Schlüter regime, the tokamak banana regime, and the ripple regime are given, respectively, by

$$S^*_{PS} = 1/L^*, \qquad S^*_B \approx A^{3/2}/L^*, \qquad S^*_R = 1.65\ \delta_e^{3/2} L^*, \tag{10}$$

which are equivalent to the equations for the transport coefficients [see Eq. (4)].

In the so-called ν regime the following relation holds[5,6]:

$$S_\nu \approx \frac{v}{\Lambda} = \nu\ , \tag{11}$$

ν being the collision frequency.

Figure 7 gives results for an $\ell = 2$ stellarator for various values of Q_ℓ.

Equation (11) can be divided by Eq. (9) with the result

$$S^*_\nu = H_c^2\ \nu^* \tag{12}$$

with $H_c = 0.53\ \iota\ Q_\ell$.

V. LOCAL TRANSPORT COEFFICIENTS AND MAXWELLIAN DISTRIBUTION

The results obtained for a monoenergetic particle distribution can be convoluted with a Maxwellian energy distribution:

$$f(E)\,\mathrm{d}E = \frac{2}{\sqrt{\pi}} \left(\frac{E}{kT}\right)^{1/2} \exp\left(-\frac{E}{kT}\right) \frac{\mathrm{d}E}{kT}, \tag{13}$$

or

$$f(v)\,\mathrm{d}v = \frac{4}{\sqrt{\pi}} \left(\frac{v}{v_\mathrm{T}}\right)^2 \exp\left(-\left(\frac{v}{v_\mathrm{T}}\right)^2\right) \frac{\mathrm{d}v}{v_\mathrm{T}}, \tag{14}$$

with

$$E = \frac{m}{2} v^2 \quad \text{and} \quad kT = \frac{m}{2} v_\mathrm{T}^2.$$

With the mean energy

$$E_\mathrm{o} = \langle E \rangle = \frac{m}{2} v_\mathrm{o}^2 = \frac{3}{2} kT, \qquad v_\mathrm{o}^2 = \frac{3}{2} v_\mathrm{T}^2,$$

we can rewrite the Maxwellian distribution:

$$f(v) = \sqrt{\frac{24}{\pi}} \frac{3}{2} \left(\frac{v}{v_\mathrm{o}}\right)^2 \exp\left(-\frac{3}{2}\left(\frac{v}{v_\mathrm{o}}\right)^2\right) \frac{\mathrm{d}v}{v_\mathrm{o}}. \tag{15}$$

Here again the transport coefficient and mean free path can be normalized:

$$D^*_\mathrm{Max} = \frac{D}{D_\mathrm{o}}, \qquad D_\mathrm{o} = 0.64 \frac{\varrho_\mathrm{o}^2\, v_\mathrm{o}}{t\pi R_\mathrm{o}} = 0.64 \frac{m^2\, v_\mathrm{o}^3}{e^2 B_\mathrm{o}^2\, t\pi R_\mathrm{o}}, \tag{16}$$

$$L^*_\mathrm{o} = \frac{\Lambda_\mathrm{o}}{L_\mathrm{c}}, \quad \Lambda_\mathrm{o} = v_\mathrm{o}\, \tau_{90^\circ}(v_\mathrm{o}), \tag{17}$$

where the collision time τ_{90° is given by[13]

$$\tau_{90^\circ}(v) = \frac{v^3}{A_\mathrm{D}\,(\Phi(x) - G(x))}, \quad A_\mathrm{D} = \frac{Z^2 Z_1^2 e^4 n_1 \ln\lambda}{2\pi\, \varepsilon_\mathrm{o}^2\, m^2}, \quad x = \frac{v}{v_\mathrm{T}}, \tag{18}$$

and $(\Phi(x) - G(x))$ is available as a tabulated function[13] (for $v = v_\mathrm{o}$ we get $x = 1.225$ and $\Phi - G = 0.714$). Z, m, and v refer to test particles, Z_1 and n_1 refer to field particles, Z and Z_1 are the charge numbers of the particles.

The monoenergetic results can be convoluted to obtain the three transport coefficients which are relevant in the determination of particle and energy fluxes[14]:

$$D_1^* = \sqrt{\frac{24}{\pi}} \int \frac{D(v)}{D_o} \left(\frac{3}{2}\right) \left(\frac{v}{v_o}\right)^2 \exp\left(-\frac{3}{2}\left(\frac{v}{v_o}\right)^2\right) \frac{\mathrm{d}v}{v_o}, \tag{19}$$

$$D_2^* = \sqrt{\frac{24}{\pi}} \int \frac{D(v)}{D_o} \left(\frac{3}{2}\right)^2 \left(\frac{v}{v_o}\right)^4 \exp\left(-\frac{3}{2}\left(\frac{v}{v_o}\right)^2\right) \frac{\mathrm{d}v}{v_o}, \tag{20}$$

$$D_3^* = \sqrt{\frac{24}{\pi}} \int \frac{D(v)}{D_o} \left(\frac{3}{2}\right)^3 \left(\frac{v}{v_o}\right)^6 \exp\left(-\frac{3}{2}\left(\frac{v}{v_o}\right)^2\right) \frac{\mathrm{d}v}{v_o}, \tag{21}$$

with

$$\frac{D(v)}{D_o} = \frac{D^*(v)\ D_P(v)}{D_o} = D^*(v) \left(\frac{v}{v_o}\right)^3. \tag{22}$$

Figure 8 gives results for a tokamak without ripple in the case of monoenergetic particles (with pitch angle scattering only) and particles of a Maxwellian particle distribution (with full energy scattering, mean particle energy equal to that of the monoenergetic particles), the monoenergetic results being convoluted with a Maxwellian distribution, and — for comparison — theoretical results.[15] The theoretical formula was taken from Ref. 16.

Calculation of transport coefficients of stellarators for a Maxwellian distribution was done with the formulas for monoenergetic particles: $D^*_{\nu^{1/2}} = C_{\nu^{1/2}}\ H^{3/2}\ \sqrt{\nu^*}$, $D^*_\nu = C_\nu\ H^2\ \nu^*$ [Eq. (5)], and with $D^*_X(L^*)$ as upper limit [X = PS, B, R; Eq. (4), without electric field].

For convolution the formula

$$D^*(\nu^*) = \left(\frac{1}{D^*_X} + \frac{1}{\min(D^*_{\nu^{1/2}}, D^*_\nu)}\right)^{-1}$$

was used in the ripple regime, and

$$D^*(\nu^*) = \min(D^*_X, D^*_{\nu^{1/2}}, D^*_\nu)$$

otherwise (for smaller L^*).

The normalized transport coefficients D_1^* can be written as follows:

$$D^*_{1R} = 5.42\, D^*_R = 8.94\, C_R\, \delta_e^{3/2}\, L^*_o, \tag{23}$$

$$D^*_{1\nu^{1/2}} = 1.137\, D^*_{\nu^{1/2}} = 1.137\, C_{o\nu^{1/2}}\, H_o^{3/2} \sqrt{\nu^*_o}, \tag{24}$$

$$D^*_{1\nu} = 0.912\, D^*_\nu = 0.912\, C_{o\nu}\, H_o^2\, \nu^*_o, \tag{25}$$

with

$$\nu^*_o = \frac{1}{L^*_o}, \quad H_o = \frac{2}{A}\frac{t}{\varrho_o}\frac{E_o}{eF} = \frac{t\, a\, Q_{o\varrho}}{R_o}\frac{E_o}{e\phi_o}, \quad \varrho_o = \frac{m v_o}{e B_o}, \quad Q_{o\varrho} = \frac{a}{\varrho_o}, \tag{26}$$

and

$$C_{o\nu^{1/2}} = C_{11}\,\frac{1 + C_{12}\frac{A}{H_o^{3/2}}}{1 + \left(\frac{H_o}{H_{oc}}\right)^{3/2}}, \quad C_{o\nu} = C_{21}\,\frac{1 + C_{22}\frac{A^{3/2}}{H_o^2}}{1 + \left(\frac{H_o}{H_{oc}}\right)^2}, \quad H_{oc} \approx 0.53\,\iota\,Q_{o\ell}\,. \tag{27}$$

Figure 9 presents results for an $\ell = 2$ stellarator together with a computation using a Maxwellian particle distribution with full energy scattering. The overall agreement between convolution of a monoenergetic particle distribution with energy relaxation (instead of energy scattering) and a direct computation with full energy scattering is good. Calculation of these results from a monoenergetic particle distribution is much faster though.

When only one kind of field particles with density n_1 is taken into account for the evaluation of the mean free path, the monoenergetic results of D_R, $D_{\nu^{1/2}}$, and D_ν can be given in formulas as follows ($\gamma = \varepsilon_o^2\,(m_p)^{1/2}/e^{5/2}$, atomic weight $\mu = m/m_p$, mass of proton m_p):

$$D_R = 10.7\,C_R\,\frac{\varepsilon_o^2\,\sqrt{m}\,\delta_e^{3/2}\,E^{7/2}}{\ln\lambda\,Z^2 Z_1^2 e^6 B_o^2 R_o^2 n_1} = 10.7\,C_R\,\frac{\gamma\,\sqrt{\mu}\,\delta_e^{3/2}\,(E/e)^{7/2}}{\ln\lambda\,Z^2 Z_1^2 B_o^2 R_o^2 n_1}, \tag{28}$$

$$D_{\nu^{1/2}} = 0.290\,C_{\nu^{1/2}}\,\frac{\sqrt{\ln\lambda}\,Z\,Z_1 r^{3/2} E^{5/4}\sqrt{n_1}}{\varepsilon_o\,m^{1/4}\,F^{3/2}\,\sqrt{B_o}\,R_o^2} = 0.290\,C_{\nu^{1/2}}\,\frac{\sqrt{\ln\lambda}\,Z\,Z_1 r^{3/2}\,(E/e)^{5/4}\sqrt{n_1}}{\sqrt{\gamma}\,\mu^{1/4}\,F^{3/2}\,\sqrt{B_o}\,R_o^2}, \tag{29}$$

$$D_\nu = 0.103\,C_\nu\,\frac{\ln\lambda\,Z^2 Z_1^2 e^2 r^2\sqrt{E}\,n_1}{\varepsilon_o^2\,\sqrt{m}\,F^2\,R_o^2} = 0.103\,C_\nu\,\frac{\ln\lambda\,Z^2 Z_1^2 r^2\,(E/e)^{1/2}\,n_1}{\gamma\,\sqrt{\mu}\,F^2\,R_o^2}. \tag{30}$$

The results for a Maxwellian energy distribution can be given as follows:

$$D_{1R} = 239\,C_R\,\frac{\varepsilon_o^2\,\sqrt{m}\,\delta_e^{3/2}\,(kT)^{7/2}}{\ln\lambda\,Z^2 Z_1^2 e^6 B_o^2 R_o^2 n_1} = 239\,C_R\,\frac{\gamma\,\sqrt{\mu}\,\delta_e^{3/2}\,(kT/e)^{7/2}}{\ln\lambda\,Z^2 Z_1^2 B_o^2 R_o^2 n_1}, \tag{31}$$

$$D_{1\nu^{1/2}} = 0.548\,C_{o\nu^{1/2}}\,\frac{\sqrt{\ln\lambda}\,Z\,Z_1 r^{3/2}\,(kT)^{5/4}\sqrt{n_1}}{\varepsilon_o\,m^{1/4}\,F^{3/2}\,\sqrt{B_o}\,R_o^2} = 0.548\,C_{o\nu^{1/2}}\,\frac{\sqrt{\ln\lambda}\,Z\,Z_1 r^{3/2}\,(kT/e)^{5/4}\sqrt{n_1}}{\sqrt{\gamma}\,\mu^{1/4}\,F^{3/2}\,\sqrt{B_o}\,R_o^2}, \tag{32}$$

$$D_{1\nu} = 0.115\,C_{o\nu}\,\frac{\ln\lambda\,Z^2 Z_1^2 e^2 r^2\sqrt{kT}\,n_1}{\varepsilon_o^2\,\sqrt{m}\,F^2\,R_o^2} = 0.115\,C_{o\nu}\,\frac{\ln\lambda\,Z^2 Z_1^2 r^2\,(kT/e)^{1/2}\,n_1}{\gamma\,\sqrt{\mu}\,F^2\,R_o^2}. \tag{33}$$

For practical purposes this can be shortened to

$$D_{1R} = 4.14{\cdot}10^{26}\ C_R\ \frac{\sqrt{\mu}\ \delta_e^{3/2}\ T_4^{7/2}}{Z^2 Z_1^2\ B_o^2\ R_o^2\ n_1}\ [m^2 s^{-1}], \tag{34}$$

$$D_{1\nu^{1/2}} = 4.15{\cdot}10^{-7}\ C_{o\nu^{1/2}}\ \frac{Z\,Z_1\ r^{3/2}\ T_4^{5/4}\ \sqrt{n_1}}{\mu^{1/4}\ F_4^{3/2}\ \sqrt{B_o}\ R_o^2}\ [m^2 s^{-1}], \tag{35}$$

$$D_{1\nu} = 6.63{\cdot}10^{-18}\ C_{o\nu}\ \frac{Z^2 Z_1^2\ r^2\ \sqrt{T_4}\ n_1}{\sqrt{\mu}\ F_4^2\ R_o^2}\ [m^2 s^{-1}], \tag{36}$$

with $\ln\lambda = 18$, $\varepsilon_o = 8.854{\cdot}10^{-12}\,As/Vm$, $e = 1.602{\cdot}10^{-19}\,As$, $m_e = 9.108{\cdot}10^{-31}\,kg$, $m_p = 1.6726{\cdot}10^{-27}\,kg$, $m_D = 3.344{\cdot}10^{-27}\,kg$, $\gamma = 3.121{\cdot}10^{11}\,s/m^3V^{3/2}$, $E = 3/2\,kT$, T_4 in 10 keV, F_4 in 10 kV/m, B_o in T, R_o and r in m, n_1 in m^{-3}.

Recently Ho and Kulsrud[17] published a paper giving results for transport coefficients from a basically analytical Fokker-Planck calculation.

For electron ripple transport they find

$$D_{1R}\,n_e = 8.15{\cdot}10^{24}\ \frac{\varepsilon_h^{3/2}(r)\ T_4^{7/2}}{B_o^2\ R_o^2}\ [m^{-1}s^{-1}] \tag{37}$$

and for ion (deuteron) transport in the $\sqrt{\nu}$ regime

$$D_{1\nu^{1/2}}\,n_d = 3.81{\cdot}10^{22}\ \frac{r^{3/2}\ T_4^{5/4}\ n_{20}^{3/2}}{F_4^{3/2}\ \sqrt{B_o}\ R_o^2}\ [m^{-1}s^{-1}] \tag{38}$$

(n_{20} in $10^{20}\,m^{-3}$; the quantity $\partial\Phi/\partial r_m$ of Ho et al. is *not* in 10 kV/m but in kV/m, though the quantity $e\,\partial\Phi/\partial r_m$ *is* in 10 keV/m. $T_4^{7/4}$ instead of $T_4^{5/4}$ is a typographical error).

This is in good agreement with our results for the $\ell = 2$ stellarator ($C_R = 1.00$, $C_{o\nu^{1/2}} = 0.11 = C_{11}$, $C_{12} = 0$, $H_{oc} \to \infty$; see Table I and Table II):

$$D_{1R}\,n_e = 9.66{\cdot}10^{24}\ \frac{\delta_e^{3/2}(r)\ T_4^{7/2}}{B_o^2\ R_o^2}\ [m^{-1}s^{-1}] \tag{39}$$

(assuming electron-electron collisions only) and

$$D_{1\nu^{1/2}}\,n_d = 3.84{\cdot}10^{22}\ \frac{r^{3/2}\ T_4^{5/4}\ n_{20}^{3/2}}{F_4^{3/2}\ \sqrt{B_o}\ R_o^2}\ [m^{-1}s^{-1}]. \tag{40}$$

Ho and Kulsrud have not considered the ν regime. Here we get ($C_{o\nu} = 1.1 = C_{21}$, $C_{22} = 0$, $H_{oc} \to \infty$)

$$D_{1\nu}\,n_d = 5.15{\cdot}10^{22}\ \frac{r^2\ \sqrt{T_4}\ n_{20}^2}{F_4^2\ R_o^2}\ [m^{-1}s^{-1}]. \tag{41}$$

VI. PARTICLE FLUX, ENERGY FLUX AND CONFINEMENT TIMES

Here, we briefly repeat[17,18] the set of formulas which lead to "zero dimensional" estimates of particle and energy confinement times. These estimates are obtained at half the plasma radius with the simplest specific assumptions on density, temperature, and potential profiles.

The particle flux Γ is:

$$\Gamma = -D_1 n \left(\frac{1}{n}\frac{\partial n}{\partial r} + \frac{q}{kT}\frac{\partial \phi}{\partial r} - \frac{3}{2}\frac{1}{T}\frac{\partial T}{\partial r} + \frac{D_2}{D_1}\frac{1}{T}\frac{\partial T}{\partial r} \right) \tag{42}$$

and the energy flux

$$Q = -D_2 n kT \left(\frac{1}{n}\frac{\partial n}{\partial r} + \frac{q}{kT}\frac{\partial \phi}{\partial r} - \frac{3}{2}\frac{1}{T}\frac{\partial T}{\partial r} + \frac{D_3}{D_2}\frac{1}{T}\frac{\partial T}{\partial r} \right), \tag{43}$$

with $q = +e$ for ions and $q = -e$ for electrons.

Assuming parabolic profiles for density, temperature and potential,

$$n = n_o \left(1 - \left(\frac{r}{a}\right)^2\right), \quad T = T_o \left(1 - \left(\frac{r}{a}\right)^2\right), \quad \phi = \phi_o \left(1 - \left(\frac{r}{a}\right)^2\right), \tag{44}$$

we get for $r_o = 0.5\,a$, $n(r_o) = 0.75\,n_o$ etc. the particle flux

$$\Gamma = +\frac{D_1 n_o}{a}\left(\frac{D_2}{D_1} - \frac{1}{2} + \frac{q\phi_o}{kT_o}\right) = \frac{4}{3}\frac{D_1 n(r_o)}{a}\left(\frac{D_2}{D_1} - \frac{1}{2} + \frac{q\phi_o}{kT_o}\right) \tag{45}$$

and the energy flux

$$Q = +\frac{3}{4}\frac{D_2 n_o kT_o}{a}\left(\frac{D_3}{D_2} - \frac{1}{2} + \frac{q\phi_o}{kT_o}\right) = \frac{4}{3}\frac{D_2 n(r_o) kT(r_o)}{a}\left(\frac{D_3}{D_2} - \frac{1}{2} + \frac{q\phi_o}{kT_o}\right). \tag{46}$$

The area O of the flux surface at $r_o = 0.5\,a$ is

$$O = 2\pi^2 a R_o\,. \tag{47}$$

The volume element $\mathrm{d}V$ is

$$\mathrm{d}V = 4\pi^2 R_o r\,\mathrm{d}r \tag{48}$$

and the particle number N within this flux surface is

$$N = \int n\,\mathrm{d}V = \tfrac{7}{16}\pi^2 n_o a^2 R_o\,. \tag{49}$$

The particle confinement time τ_N is then

$$\tau_N = \frac{N}{\Gamma O} = \frac{1}{4.6}\frac{a^2}{D_1}\left(\frac{D_2}{D_1} - \frac{1}{2} + \frac{q\phi_o}{kT_o}\right)^{-1} \tag{50}$$

and the particle loss rate S_N is

$$S_N = \frac{1}{\tau_N} = 4.6\,\frac{D_1}{a^2}\left(\frac{D_2}{D_1} - \frac{1}{2} + \frac{q\phi_o}{kT_o}\right). \tag{51}$$

The energy content W within this flux surface is

$$W = \int n \tfrac{3}{2} kT \, \mathrm{d}V = \tfrac{37}{64} \pi^2 n_o \, kT_o \, a^2 \, R_o \, . \tag{52}$$

Thus, the energy confinement time τ_W is

$$\tau_W = \frac{W}{Q\,O} = \frac{1}{2.6} \frac{a^2}{D_2} \left(\frac{D_3}{D_2} - \frac{1}{2} + \frac{q\phi_o}{kT_o} \right)^{-1} \tag{53}$$

and the energy loss rate S_W is

$$S_W = \frac{1}{\tau_W} = 2.6 \frac{D_2}{a^2} \left(\frac{D_3}{D_2} - \frac{1}{2} + \frac{q\phi_o}{kT_o} \right) . \tag{54}$$

The ratios of transport coefficients D_1, D_2, and D_3 can be found in Table II.

VII. APPLICATION TO VARIOUS STELLARATORS

Figures 10 to 15 give results for Maxwellian energy distributions for various configurations: $\ell = 2$ stellarator, W VII-AS, Helias49, TJ-II, ATF and Heliotron-E.

From figures of this type sets of consistent parameters can be derived in the long mean free path regime. The following definitions have been used: Plateau value of the transport coefficient $D_o = 0.64 \varrho_o^2 v_o / \iota \pi R_o$, plateau value of the loss rate $S_o = 5.7 D_o / a^2$, plateau value of the confinement time $\tau_o = 1/S_o$, ratio of the electric potential to the mean energy $C_\phi = q\phi_o / E_o(r_o)$, $\phi = \phi_o (1 - r^2/a^2)$. Three additional confinement times are defined as follows:

$$\tau_1 = \frac{a^2}{5.7 D_1}, \quad \tau_2 = \frac{a^2}{4.6 D_2}, \quad \text{and} \quad \tau_3 = \frac{a^2}{2.6 D_3}. \tag{55}$$

The particle confinement time is $\tau_N \approx \tau_2$ and the energy confinement time is $\tau_W \approx \tau_3$ as long as the quantity $-1/2 + q\phi_o / kT_o$ in Eqs. (50) and (53) can be neglected. This procedure slightly overestimates the electron confinement times and slightly underestimates the ion confinement times in the case of a potential $\phi_o < 0$ which is attractive for ions and repulsive for electrons.

In the following is $C_\phi = \pm 1$ arbitraryly, and the confinement times τ_1, τ_2, and τ_3 were taken from those D^* values where $D^*_{ke} = D^*_{ki}$ for $k = 1, 2, 3$. The value of L^*_o was chosen accordingly, and thus the values for $n_e = n_i$ and $\beta = 2\mu_o 2 n_e kT / B_o^2$ can be derived with $T_e = T_i = T$. This procedure is suggested by the condition of quasineutrality ($\tau_{2e} \approx \tau_{2i}$), which is thus incorporated in a consistent though primitive way compatible with the long mean free path regime.

W VII-AS[8]: $R_o = 2$ m, $a = 0.2$ m, $A = 20$, $r_o = 0.1$ m, $\iota(r_o) = 0.389$, $L_c = 16.2$ m, $B_o = 3$ T, $kT(r_o) = 2$ keV, $E_o = 3$ keV, $v_o = 5.36 \cdot 10^5$ m/s (deuterons), $\varrho_o = 3.73 \cdot 10^{-3}$ m, $Q_{o\varrho} = 54$, $\beta(r_o) = 0.5\%$, $n_e(r_o) = 2.8 \cdot 10^{19}$ m^{-3}, $\Lambda_o = 1.9 \cdot 10^3$ m, $L^*_o = 119$, $D_o = 1.95$ m^2/s, $S_o = 278$ s^{-1}, $C_\phi = \pm 1$, $\tau_o = 4$ ms, $\tau_1 = 67$ ms, $\tau_2 = 24$ ms, $\tau_3 = 10$ ms.
With protons instead of deuterons, the following values are different: $v_o = 7.58 \cdot 10^5$ m/s, $\varrho_o = 2.64 \cdot 10^{-3}$ m, $Q_{o\varrho} = 76$, $D_o = 1.38$ m^2/s, $S_o = 197$ s^{-1}, $\tau_o = 5$ ms, $\tau_1 = 67$ ms, $\tau_2 = 25$ ms, $\tau_3 = 10$ ms.

Helias49[9]: $R_o = 5$ m, $a = 0.5$ m, $A = 20$, $r_o = 0.25$ m, $\iota(r_o) = 0.746$, $L_c = 21.1$ m, $B_o = 4$ T, $kT(r_o) = 6.4$ keV, $E_o = 9.6$ keV, $v_o = 9.59 \cdot 10^5$ m/s (deuterons), $\varrho_o = 5 \cdot 10^{-3}$ m, $Q_{o\varrho} = 100$, $\beta(r_o) = 2\%$, $n_e(r_o) = 6.2 \cdot 10^{19}$ m^{-3}, $\Lambda_o = 8.9 \cdot 10^3$ m, $L^*_o = 420$, $D_o = 1.31$ m^2/s, $S_o = 30$ s^{-1}, $C_\phi = \pm 1$, $\tau_o = 33$ ms, $\tau_1 = 0.89$ s, $\tau_2 = 0.36$ s, $\tau_3 = 0.17$ s.

TJ-II[10]: $R_o = 1.5$ m, $a = 0.2$ m, $A = 15$, $r_o = 0.1$ m, $\iota(r_o) = 1.477$, $L_c = 3.19$ m, $B_o = 1$ T, $kT(r_o) = 0.2$ keV, $E_o = 0.3$ keV, $v_o = 1.70 \cdot 10^5$ m/s (deuterons), $\varrho_o = 3.54 \cdot 10^{-3}$ m, $Q_{o\varrho} = 56$, $\beta(r_o) = 0.1\%$, $n_e(r_o) = 0.62 \cdot 10^{19}$ m^{-3}, $\Lambda_o = 87$ m, $L^*_o = 27$, $D_o = 0.195$ m^2/s, $S_o = 28$ s^{-1}, $C_\phi = \pm 1$, $\tau_o = 36$ ms, $\tau_1 = 27$ ms, $\tau_2 = 11$ ms, $\tau_3 = 5$ ms.
With protons instead of deuterons, the following values are different: $v_o = 2.40 \cdot 10^5$ m/s,

$\varrho_o = 2.50 \cdot 10^{-3}$ m, $Q_{o\varrho} = 80$, $D_o = 0.138$ m^2/s, $S_o = 20$ s^{-1}, $\tau_o = 51$ ms, $\tau_1 = 26$ ms, $\tau_2 = 11$ ms, $\tau_3 = 5$ ms.

ATF[11]: $R_o = 2.1$ m, $a = 0.3$ m, $A = 14$, $r_o = 0.15$ m, $\iota(r_o) = 0.425$, $L_c = 15.5$ m, $B_o = 2$ T, $kT(r_o) = 2$ keV, $E_o = 3$ keV, $v_o = 5.36 \cdot 10^5$ m/s (deuterons), $\varrho_o = 5.60 \cdot 10^{-3}$ m, $Q_{o\varrho} = 54$, $\beta(r_o) = 2\%$, $n_e(r_o) = 5.0 \cdot 10^{19}$ m^{-3}, $\Lambda_o = 1.08 \cdot 10^3$ m, $L_o^* = 70$, $D_o = 3.84$ m^2/s, $S_o = 243$ s^{-1}, $C_\phi = \pm 1$, $\tau_o = 4$ ms, $\tau_1 = 20$ ms, $\tau_2 = 8$ ms, $\tau_3 = 4$ ms.
With protons instead of deuterons, the following values are different: $v_o = 7.58 \cdot 10^5$ m/s, $\varrho_o = 3.96 \cdot 10^{-3}$ m, $Q_{o\varrho} = 76$, $D_o = 2.71$ m^2/s, $S_o = 172$ s^{-1}, $\tau_o = 6$ ms, $\tau_1 = 21$ ms, $\tau_2 = 9$ ms, $\tau_3 = 4$ ms.

Heliotron-E[12]: $R_o = 2.2$ m, $a = 0.2$ m, $A = 16.7$, $r_o = 0.132$ m, $\iota(r_o) = 1.032$, $L_c = 6.7$ m, $B_o = 2$ T, $kT(r_o) = 0.667$ keV, $E_o = 1$ keV, $v_o = 3.10 \cdot 10^5$ m/s (deuterons), $\varrho_o = 3.23 \cdot 10^{-3}$ m, $Q_{o\varrho} = 62$, $\beta(r_o) = 0.1\%$, $n_e(r_o) = 0.74 \cdot 10^{19}$ m^{-3}, $\Lambda_o = 0.81 \cdot 10^3$ m, $L_o^* = 121$, $D_o = 0.29$ m^2/s, $S_o = 41$ s^{-1}, $C_\phi = \pm 1$, $\tau_o = 24$ ms, $\tau_1 = 0.10$ s, $\tau_2 = 40$ ms, $\tau_3 = 17$ ms.
With protons instead of deuterons, the following values are different: $v_o = 4.38 \cdot 10^5$ m/s, $\varrho_o = 2.28 \cdot 10^{-3}$ m, $Q_{o\varrho} = 88$, $D_o = 0.205$ m^2/s, $S_o = 29$ s^{-1}, $\tau_o = 34$ ms, $\tau_1 = 0.10$ s, $\tau_2 = 39$ ms, $\tau_3 = 17$ ms.

VIII. CONCLUSIONS

It has been shown that computation of transport coefficients with a Maxwellian particle distribution and full energy scattering can be replaced by computation of a monoenergetic particle distribution with pitch angle scattering and energy relaxation only. Convolution of the monoenergetic results with a Maxwellian distribution gives essentially the same result as direct computation with full energy scattering.

The results also agree with analytical results for the axisymmetric case (see Fig. 8) and, in the appropiate limiting cases, with analytical results for the $\ell = 2$ stellarator (see Fig. 9). The latter results also appear to indicate that a less idealized analytic calculation for the $\ell = 2$ stellarator would be desirable. As evident from Fig. 9, such a calculation should incorporate plateau effects and the effect of the electric field on the electrons.

Zero-dimensional estimates of confinement have also been obtained. They indicate that neoclassical energy confinement is crucial to stellarators and should certainly be evaluated in a more complete way than has been done here. In particular, it seems that the simplified zero-dimensional procedure used here to satisfy the quasineutrality conditions can be extended to a one-dimensional one which yields $n_i(r) = n_e(r)$, $\Gamma_i(r) = \Gamma_e(r)$, and the associated electric field $F(r)$.

IX. REFERENCES

[1] A.H. Boozer, G. Kuo-Petravic, Phys. Fluids **24**, 851 (1981).

[2] R.H. Fowler, J.A. Rome, and J.F. Lyon, Phys. Fluids **28**, 338 (1985).

[3] W. Lotz and J. Nührenberg, Z. Naturforsch. **37a**, 899 (1982).

[4] W. Dommaschk, W. Lotz, and J. Nührenberg, Nucl. Fusion **24**, 794 (1984).

[5] W. Lotz, *8th Europhysics Conf. on Comp. Physics,* Eibsee 1986, Europhysics Conf. Abstracts, Vol. **10D**, 105 (1986).

[6] W. Lotz, J. Nührenberg, and A. Schlüter, J. Comput. Phys. **73**, 73 (1987).

[7] W. Lotz, J. Nührenberg, and A. Schlüter, Z. Naturforsch. **42a**, 1045 (1987).

[8] U. Brossmann, W. Dommaschk, F. Herrnegger, G. Grieger, J. Kisslinger, W. Lotz, J. Nührenberg, F. Rau, H. Renner, H. Ringler, J. Sapper, A. Schlüter, and H. Wobig, *Proc. 9th int. Conf. on Plasma Physics and Controlled Nuclear Fusion Research, Baltimore 1982,* IAEA-CN-41/Q-5, Nucl. Fusion Suppl. 1983, Vol. **III**, 141 (1983).

[9] J. Nührenberg and R. Zille, *Proc. of invited Papers of the Workshop on Theory of Fusion Plasmas, Varenna 1987,* Nuovo Cimento (1987) in press.

[10] A. Perea, J.L. Alvarez Rivas, J. Botija, J.R. Cepero, J.A. Fábregas, J. Guasp, A. López Fraguas, R. Martín, A. Pérez Navarro, A. Pueblas, E. Rodriguez Solano, B.A. Carreras, K.K. Chipley, T.C. Hender, T.C. Jernigan, J.F. Lyon, and B.E. Nelson, *Proc. 12th European Conf. on Controlled Fusion and Plasma Physics, Budapest 1985,* Europhysics Conf. Abstracts, Vol. **9 F**, Part I, 433 (1985).

[11] J.F. Lyon, B.A. Carreras, J.H. Harris, J.A. Rome, L.A. Charlton, R.A. Dory, R.H. Fowler, L. Garcia, D.L. Goodman, T.C. Hender, H.R. Hicks, S.P. Hirshman, S.A. Hokin, J.A. Holmes, T.C. Jernigan, V.E. Lynch, B.F. Masden, and J. Sheffield, *Proc. 9th int. Conf. on Plasma Physics and Controlled Nuclear Fusion Research, Baltimore 1982,* IAEA-CN-41/Q-3, Nucl. Fusion Suppl. 1983, Vol. **III**, 115 (1983).

[12] K. Uo, A. Iiyoshi, T. Obiki, O. Motojima, S. Morimoto, A. Sasaki, K. Kondo, M. Sato, T. Mutoh, H. Zushi, H. Kaneko, S. Besshou, F. Sano, T. Mizuuchi, S. Sudo, K. Hanatani, M. Nakasuga, I. Ohtake, M. Iima, Y. Nakashima, and N. Nishino, *Proc. 9th int. Conf. on Plasma Physics and Controlled Nuclear Fusion Research, Baltimore 1982,* IAEA-CN-41/L-3, Nucl. Fusion Suppl. 1983, Vol. **II**, 209 (1983).

[13] L. Spitzer, *Physics of Fully Ionized Gases* (Interscience Publishers, New York, 1956) p.77.

[14] M.N. Rosenbluth, R.D. Hazeltine, and F.L. Hinton, Phys. Fluids **15**, 116 (1972).

[15] F.L. Hinton and R.D. Hazeltine, Rev. Mod. Phys. **48**, 239 (1976).

[16] R.H. Fowler, J.A. Rome, and J.F. Lyon, Phys. Fluids **28**, 338 (1985).

[17] D. D.-M. Ho and R.M. Kulsrud, Phys. Fluids **30**, 442 (1987).

[18] E.A. Frieman, Phys. Fluids **13**, 490 (1970).

X. TABLES

TABLE I. Constants C_{ik} used in Eqs. (6), (7), and (27).

	C_{11}	C_{12}	C_{21}	C_{22}	$C_{21}\cdot C_{22}$
$\ell = 2$ Stellarator (DOM25)	0.11	1.9	1.1	0.7	0.8
W VII-AS	0.09	1.0	1.0	0.7	0.7
Helias49	0.022	3.0	0.32	1.3	0.42
TJ-II	0.33	0.5	2.8	0.25	0.7
ATF	0.18	0.8	1.9	0.3	0.6
Heliotron-E	0.20	1.0	1.8	0.25	0.45

TABLE II. Ratios of transport coefficients D_1, D_2, and D_3 used in Sec. VI derived in this paper and by Ho and Kulsrud.[17]

	Ripple regime		$\sqrt{\nu}$ regime		ν regime	
	This paper	Ref. 17	This paper	Ref. 17	This paper	Ref. 17
$\frac{D_1}{D_{\text{mono}}}$	5.42	...	1.137	...	0.912	...
$\frac{D_2}{D_1}$	4.86	4.94	2.86	2.84	2.25	...
$\frac{D_3}{D_2}$	5.89	5.95	3.83	3.82	3.19	...

XI. FIGURE CAPTIONS

FIG. 1. Normalized transport coefficients D^* for three configurations at $A = 10$, $\iota = 0.5$:
upper curve: - - - $\ell = 2$ stellarator (DOM2A), $\delta_e = 8.4\%$, $N = 10$,
middle curve: — rippled tokamak with $\delta_e = 8.4\%$,
lower curve: - · - tokamak without ripple.
The dotted lines represent D^*_R, D^*_B, and D^*_{PS}.

FIG. 2. Normalized transport coefficients D^* in an $\ell = 2$ stellarator (DOM25) for various values of Q_ℓ and electric fields. $A = 12.5$, $N = 5$, $\iota = 0.475$, $\delta_e \approx 0.03$.
$(\times)$: $Q_\ell = 2{\cdot}10^4$, $e\phi_o/E = 0$.
$(\triangle)$: $Q_\ell = 1{\cdot}10^3$, $e\phi_o/E = +1$, $H = 54.8$, $H_c = 252$.
$(\triangledown)$: $Q_\ell = 1{\cdot}10^3$, $e\phi_o/E = -1$, $H = 54.8$, $H_c = 252$.
$(\diamond)$: $Q_\ell = 1{\cdot}10^3$, $e\phi_o/E = \pm 2$, $H = 27.4$, $H_c = 252$.
$(\bigcirc)$: $Q_\ell = 1{\cdot}10^3$, $e\phi_o/E = \pm 5$, $H = 11.0$, $H_c = 252$.
$(\square)$: $Q_\ell = 1{\cdot}10^3$, $e\phi_o/E = \pm 20$, $H = 2.74$, $H_c = 252$.
The dotted lines represent $D^*_{\nu^{1/2}}$ and D^*_ν given by the respective formulas using the calculated C_{ik} .

FIG. 3. Normalized transport coefficients D^* in an $\ell = 2$ stellarator (DOM25) for various values of Q_ℓ and electric fields, $A = 25$, $N = 5$, $\iota = 0.438$, $\delta_e \approx 0.01$.
$(\times)$: $Q_\ell = 2{\cdot}10^4$, $e\phi_o/E = 0$.
$(\diamond)$: $Q_\ell = 4{\cdot}10^3$, $e\phi_o/E = \pm 2.5$, $H = 80.8$, $H_c = 929$.
$(\bigcirc)$: $Q_\ell = 2{\cdot}10^3$, $e\phi_o/E = \pm 5$, $H = 20.2$, $H_c = 464$.
$(\square)$: $Q_\ell = 1{\cdot}10^3$, $e\phi_o/E = \pm 20$, $H = 2.53$, $H_c = 232$.
The dotted lines represent $D^*_{\nu^{1/2}}$ and D^*_ν given by the respective formulas using the calculated C_{ik} .

FIG. 4. Normalized transport coefficients D^* for the W VII-AS stellarator for various values of Q_ℓ and electric fields, $A = 20$, $N = 5$, $\iota = 0.389$, $\delta_e \approx 0.03$.
$(\times)$: $Q_\ell = 2{\cdot}10^4$, $e\phi_o/E = 0$.
$(\diamond)$: $Q_\ell = 1{\cdot}10^4$, $e\phi_o/E = \pm 8$, $H = 41.6$, $H_c = 2060$.
$(\bigcirc)$: $Q_\ell = 1{\cdot}10^4$, $e\phi_o/E = \pm 16$, $H = 20.8$, $H_c = 2060$.
$(\square)$: $Q_\ell = 1{\cdot}10^3$, $e\phi_o/E = \pm 10$, $H = 3.33$, $H_c = 206$.
The dotted lines represent $D^*_{\nu^{1/2}}$ and D^*_ν given by the respective formulas using the calculated C_{ik} .

FIG. 5. Normalized transport coefficients D^* for the Helias49 stellarator for various values of Q_ℓ and electric fields, $A = 20$, $N = 4$, $\iota = 0.746$, $\delta_e \approx 0.01$.
$(\times)$: $Q_\ell = 2{\cdot}10^4$, $e\phi_o/E = 0$.
$(\diamond)$: $Q_\ell = 5{\cdot}10^3$, $e\phi_o/E = \pm 2$, $H = 180$, $H_c = 1977$.
$(\bigcirc)$: $Q_\ell = 2{\cdot}10^3$, $e\phi_o/E = \pm 4$, $H = 36.1$, $H_c = 791$.
$(\square)$: $Q_\ell = 1{\cdot}10^3$, $e\phi_o/E = \pm 10$, $H = 7.22$, $H_c = 395$.
The dotted lines represent $D^*_{\nu^{1/2}}$ and D^*_ν given by the respective formulas using the calculated C_{ik} .

FIG. 6. Normalized transport coefficients D^* for the TJ-II stellarator for various values of Q_ϱ and electric fields, $A = 15$, $N = 4$, $\iota = 1.477$, $\delta_e \approx 0.3$.
$(\times)$: $Q_\varrho = 2{\cdot}10^4$, $e\phi_o/E = 0$.
$(\diamond)$: $Q_\varrho = 2{\cdot}10^3$, $e\phi_o/E = \pm 5$, $H = 51.6$, $H_c = 1566$.
$(\circ)$: $Q_\varrho = 1{\cdot}10^3$, $e\phi_o/E = \pm 10$, $H = 12.9$, $H_c = 783$.
$(\square)$: $Q_\varrho = 5{\cdot}10^2$, $e\phi_o/E = \pm 20$, $H = 3.22$, $H_c = 391$.
The dotted lines represent $D^*_{\nu^{1/2}}$ and D^*_ν given by the respective formulas using the calculated C_{ik} .

FIG. 7. Loss rates S in an $\ell = 2$ stellarator (DOM25) for
$(\circ)$: $Q_\varrho = 50$, $B_o = 0.88$T;
$(\square)$: $Q_\varrho = 200$, $B_o = 3.5$T;
$(\diamond)$: $Q_\varrho = 1000$, $B_o = 17.6$T.
$R_o/a = 8.6$, $N = 5$, $\iota = 0.5$, $\delta_e \approx 0.02$ (at aspect ratio $A = 17$), $R_o = 10$ m, $E = 10$ keV (deuterons). The dotted line represents $S_\nu \approx \nu$.

FIG. 8. Normalized transport coefficients D^* for a tokamak with aspect ratio $A = 10$. Monoenergetic results $(\square)$ and results using a Maxwellian energy distribution with full energy scattering $(\circ)$ are shown. The continuous curve was computed by convoluting the monoenergetic results with a Maxwellian energy distribution. The dashed curve was computed by using the theoretical values of Hazeltine et al.[15,16] The dotted line on the left-hand side represents $D^*_B = A^{3/2}/L^*$.

FIG. 9. Normalized transport coefficients D^* for ion and electron particle transport (—) calculated by convoluting the monoenergetic results with a Maxwellian energy distribution. Shown are results obtained for an $\ell = 2$ stellarator (DOM25) at $A = 12.5$ with $e\phi_o/E_o = 10$ and $Q_{o\varrho} = a/\varrho_o = 10^3$ for deuterons and $Q_{o\varrho} = 6{\cdot}10^4$ for electrons, $\varrho_o = mv_o/eB_o$.
Further results were obtained by using a Maxwellian energy distribution with full energy scattering for ions $(\square)$ and for electrons $(\circ)$.
The dotted lines represent D_{1R}, $D_{1\nu^{1/2}}$, and $D_{1\nu}$, it being assumed that $C_{12} = 0$ and $C_{22} = 0$. The dotted lines are equivalent to the results of Ho and Kulsrud.[17]

FIG.10. Transport coefficients D^*_1 (—), D^*_2 (- - -), and D^*_3 (- · -) obtained for the $\ell = 2$ stellarator (DOM25) at $A = 12.5$ with $Q_{o\varrho} = 100$ (deuterons), $Q_{o\varrho} = 6{\cdot}10^3$ (electrons), and $e\phi_o/E_o = 1$. Dotted lines represent $D^*_B = A^{3/2}/L^*$ and $D^*_{\nu c} = C_{21} H_c^2 \nu^*$, which, in turn, corresponds to $S_\nu = \nu$.

FIG.11. Transport coefficients D^*_1, D^*_2, and D^*_3 obtained for the W VII-AS stellarator at $A = 20$. For further information see Fig. 10.

FIG.12. Transport coefficients D^*_1, D^*_2, and D^*_3 obtained for the Helias49 stellarator at $A = 20$. For further information see Fig. 10.

FIG.13. Transport coefficients D^*_1, D^*_2, and D^*_3 obtained for the TJ-II stellarator at $A = 15$. For further information see Fig. 10.

FIG.14. Transport coefficients D^*_1, D^*_2, and D^*_3 obtained for the ATF stellarator at $A = 14$. For further information see Fig. 10.

FIG.15. Transport coefficients D^*_1, D^*_2, and D^*_3 obtained for Heliotron-E at $A = 17$. For further information see Fig. 10.

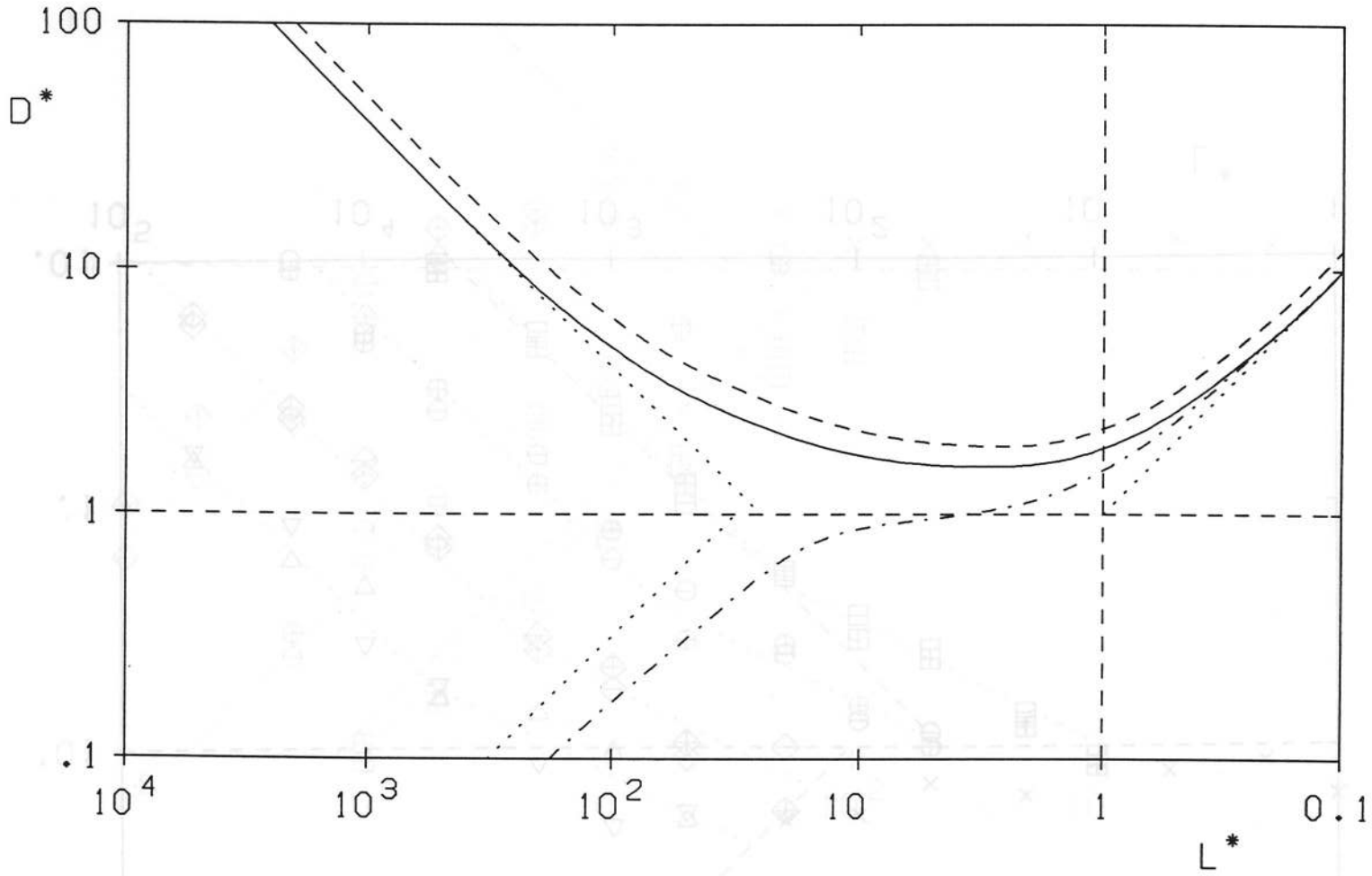

FIG. 1 Tokamak and Stellarator

REG:ZWEG.JTOKRIP

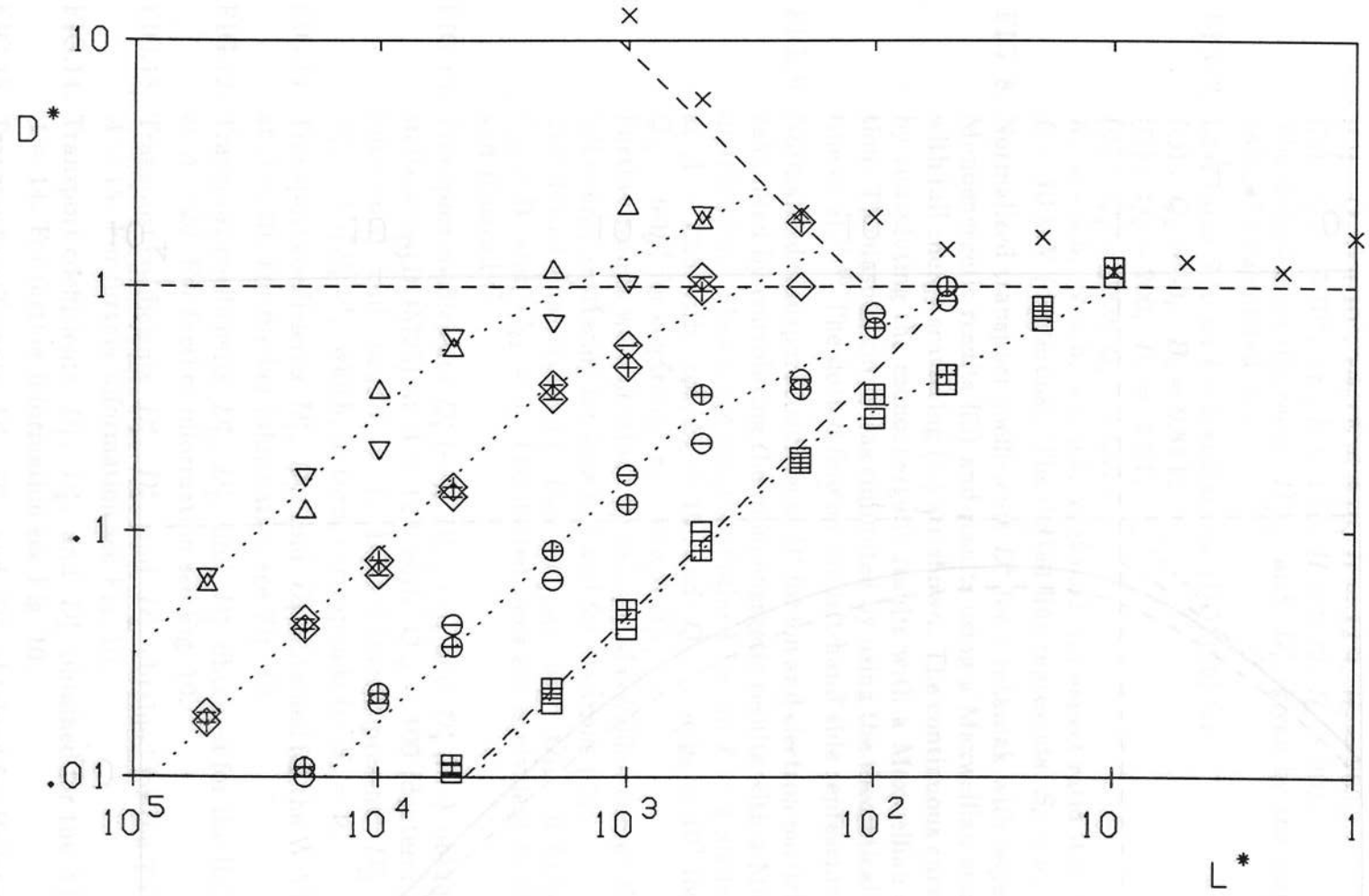

FIG. 2 l=2 Stellarator DOM25

REG:ZWEG.JDOM25DA

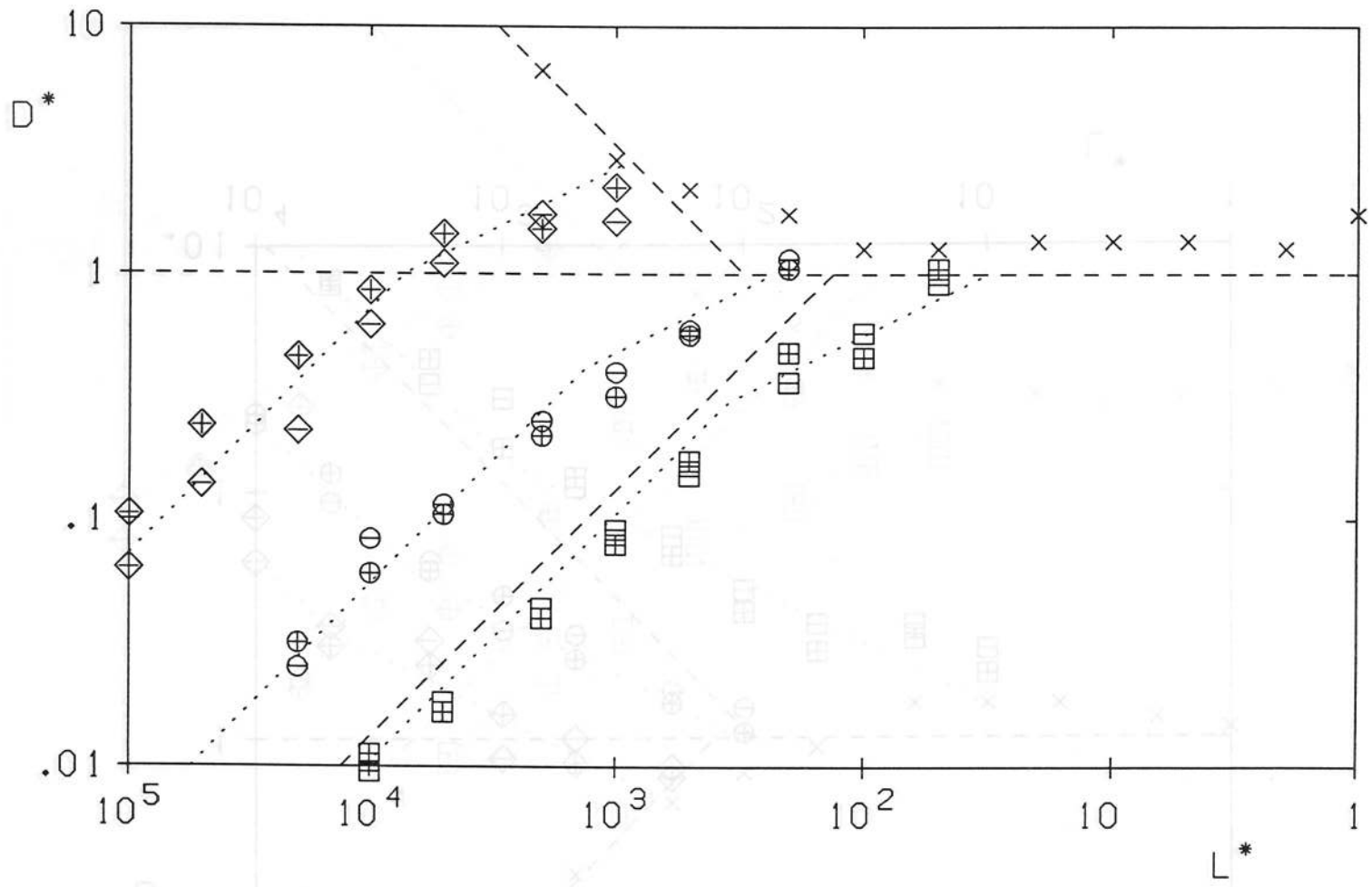

FIG. 3 l=2 Stellarator DOM25

REG:ZWEG.JDOM25DB

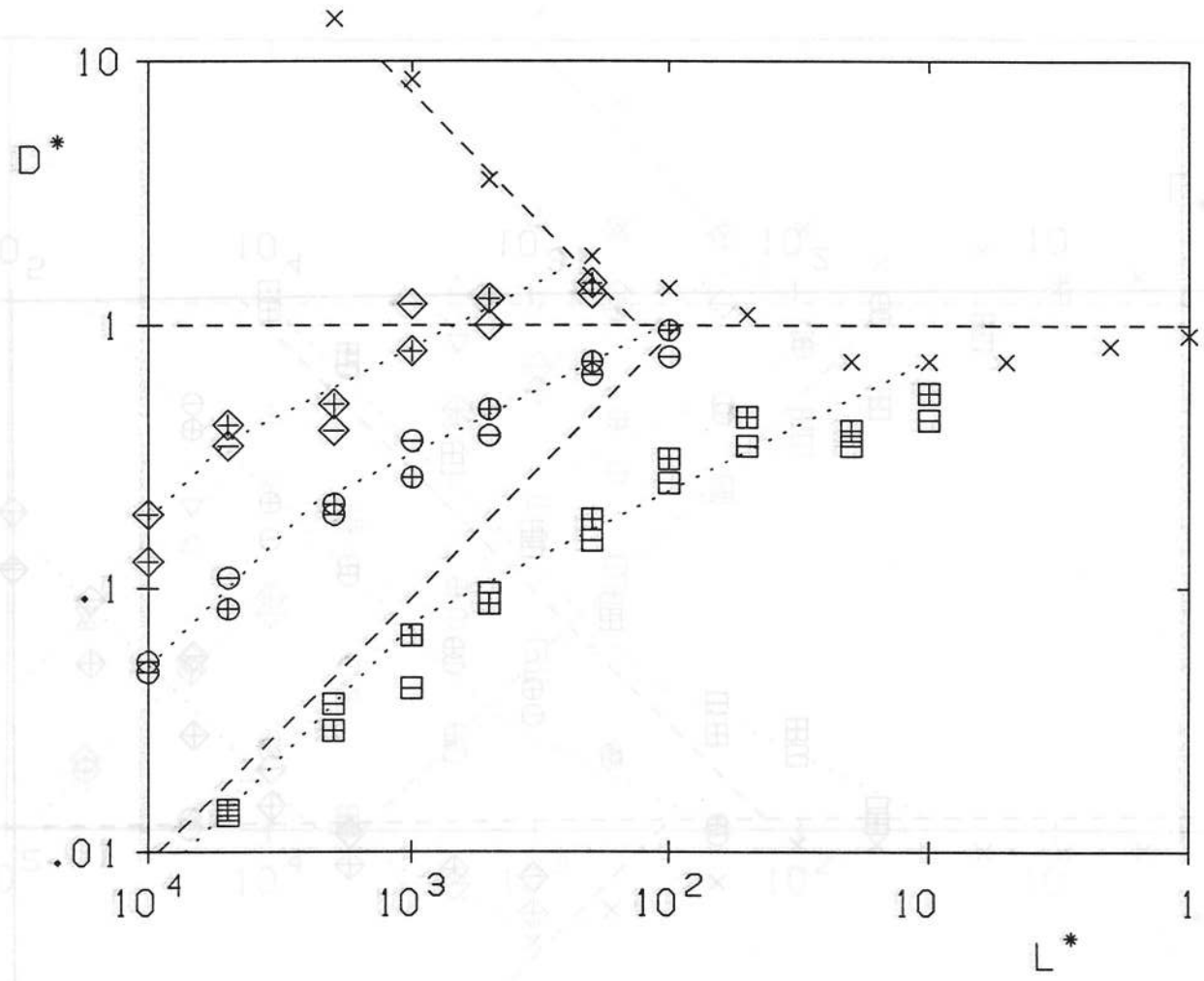

FIG. 4 Stellarator W VII-AS

REG:ZWEG.JW7ASD20

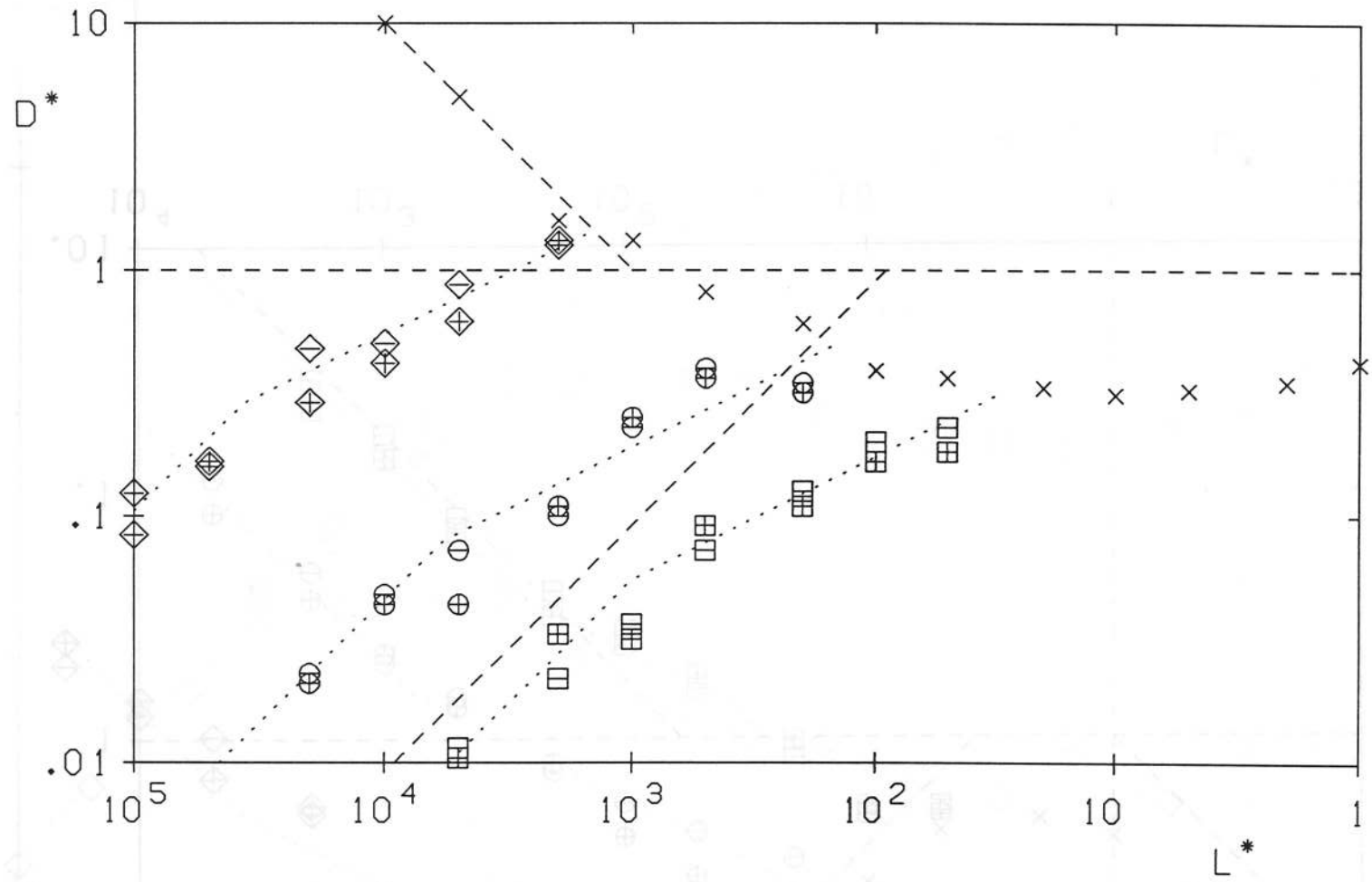

FIG. 5 Stellarator Helias49

REG:ZWEG.JHEL49

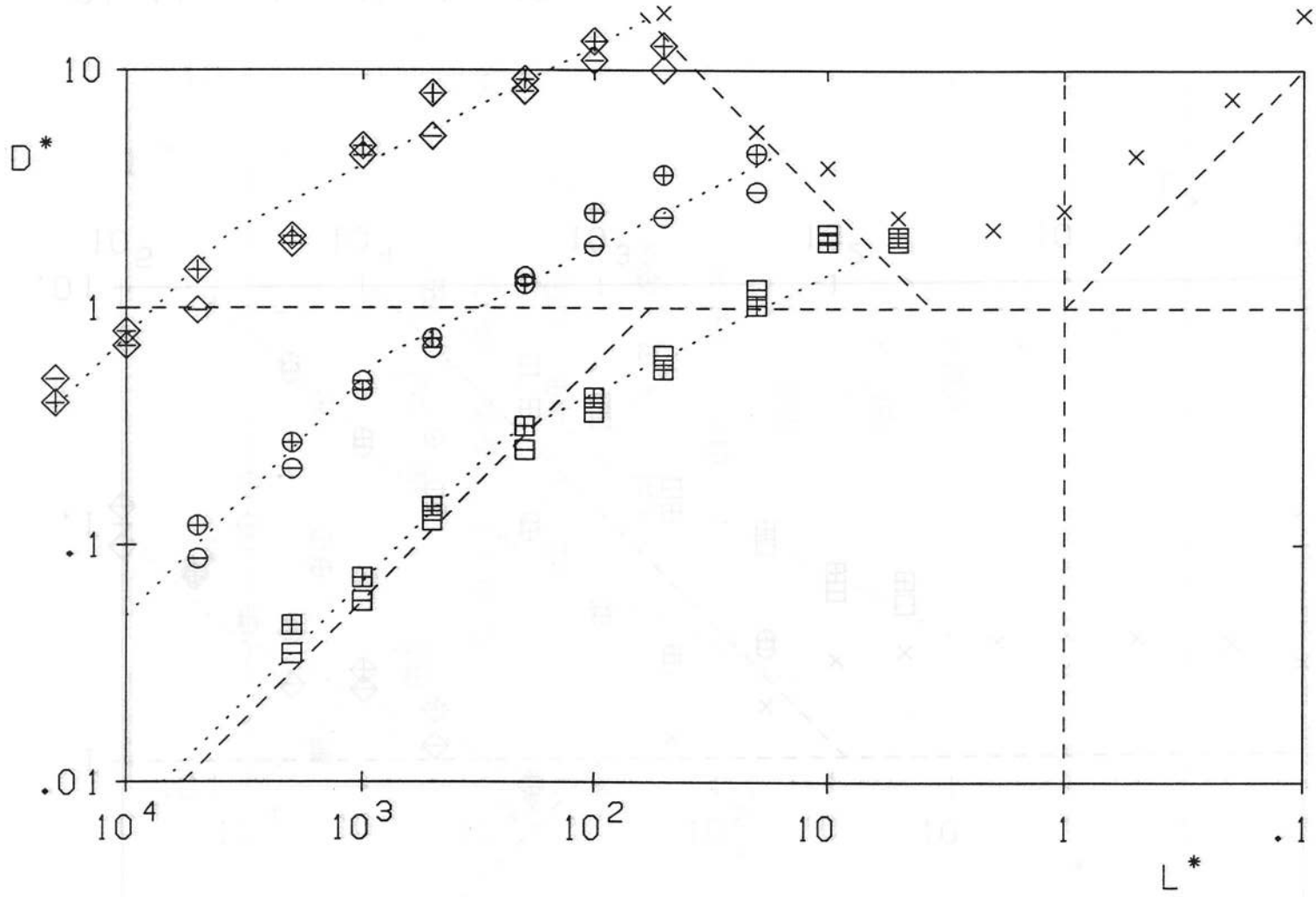

FIG. 6 Stellarator TJ-II

REG:ZWEG.JTJ2D15

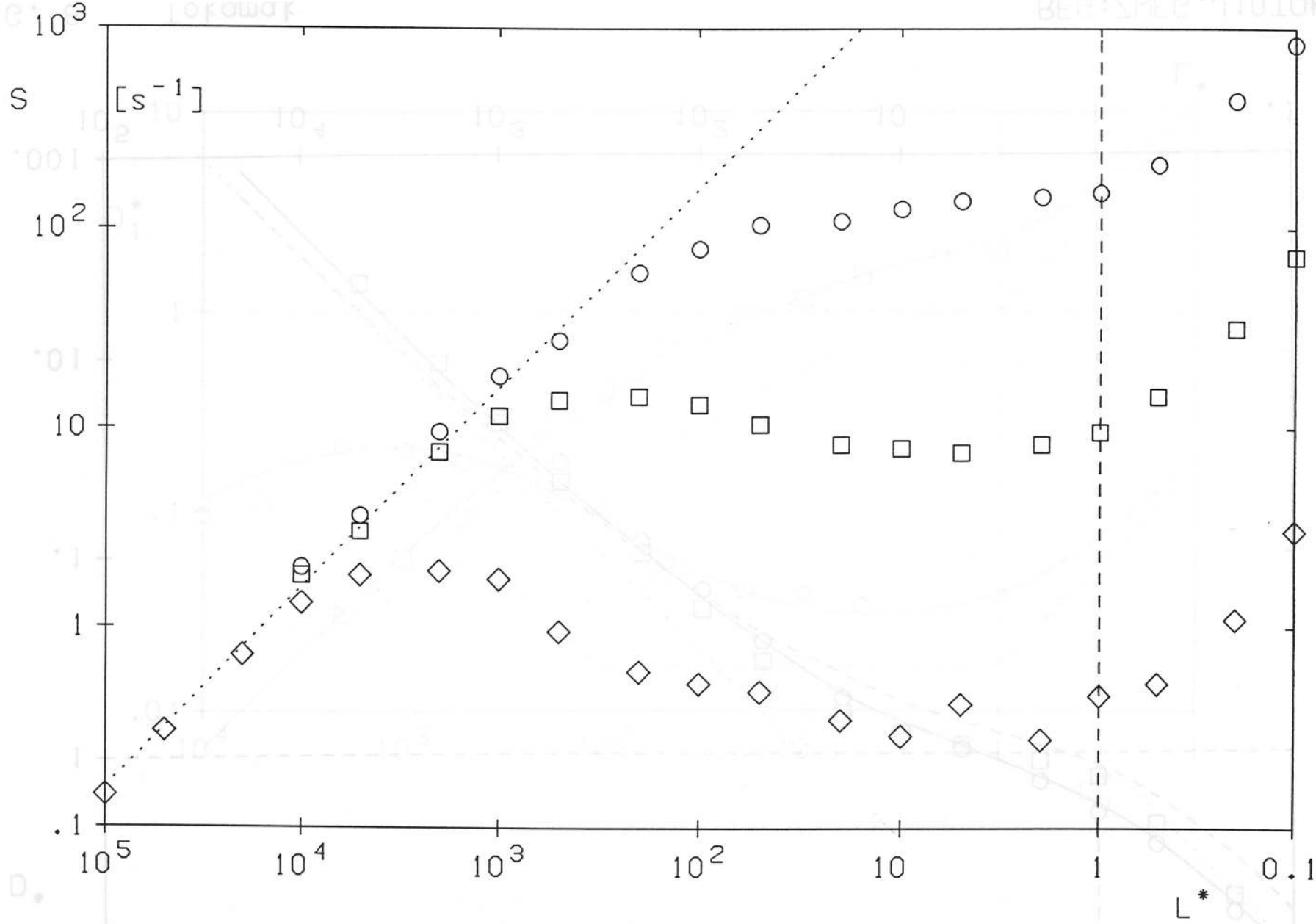

FIG. 7: l=2 Stellarator DOM25

REG:ZWEG.DOM25CS2

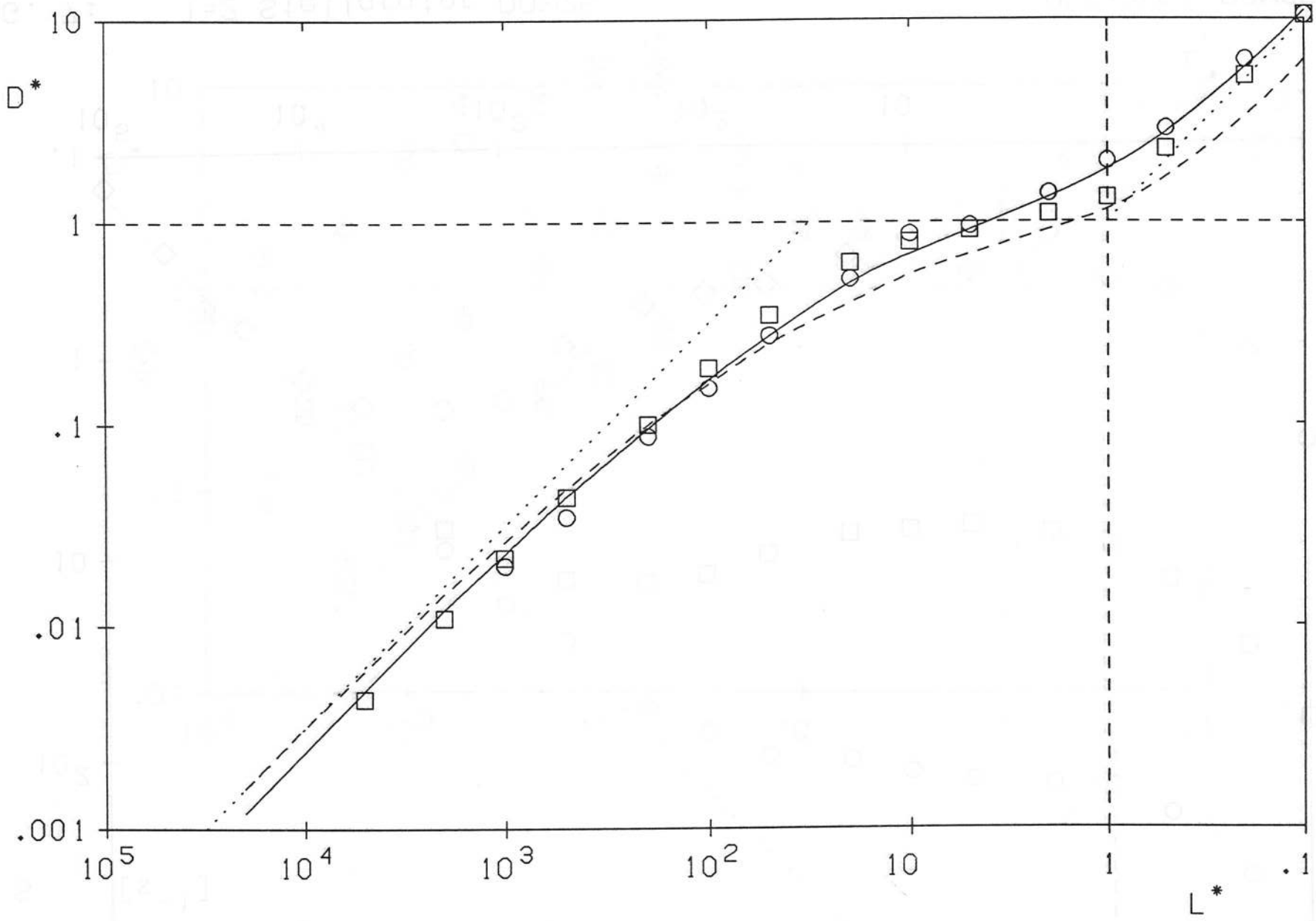

FIG. 8 Tokamak

REG:ZWEG.J10TOK

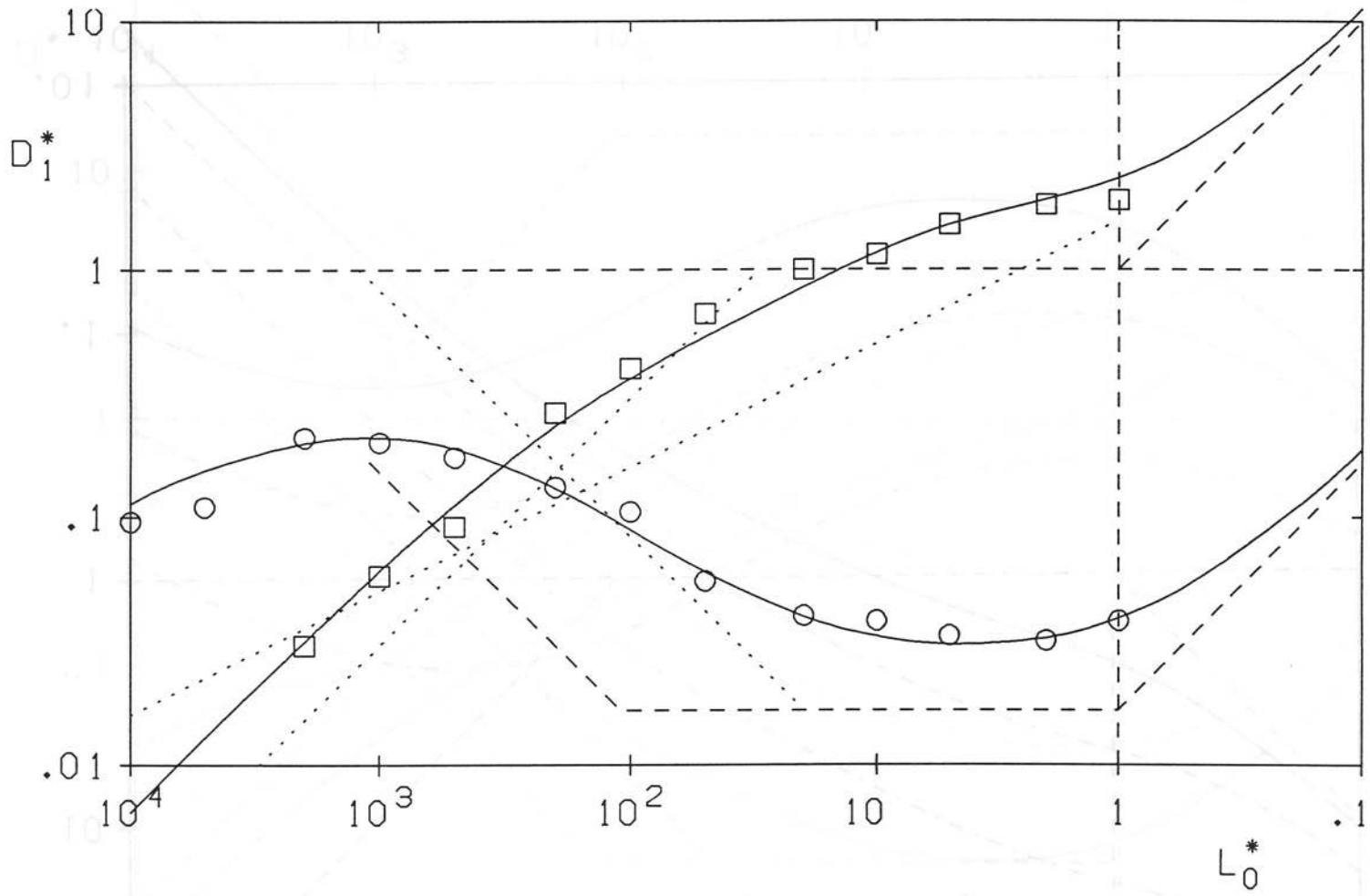

FIG. 9 l=2 Stellarator DOM25 ZOL:MAX.JDOM25A

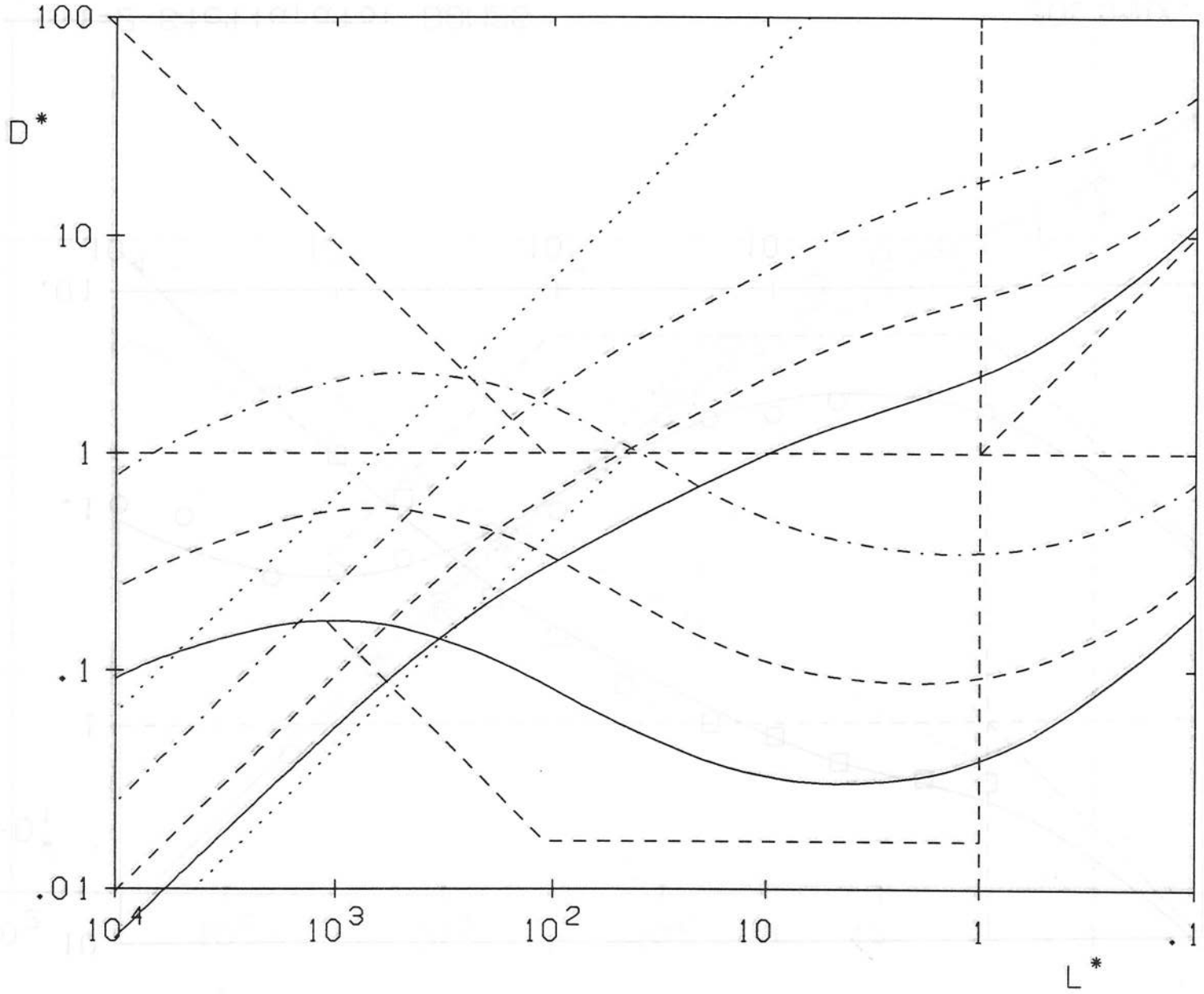

FIG. 10 l=2 Stellarator DOM25

ZOL:MAX.JDOM25

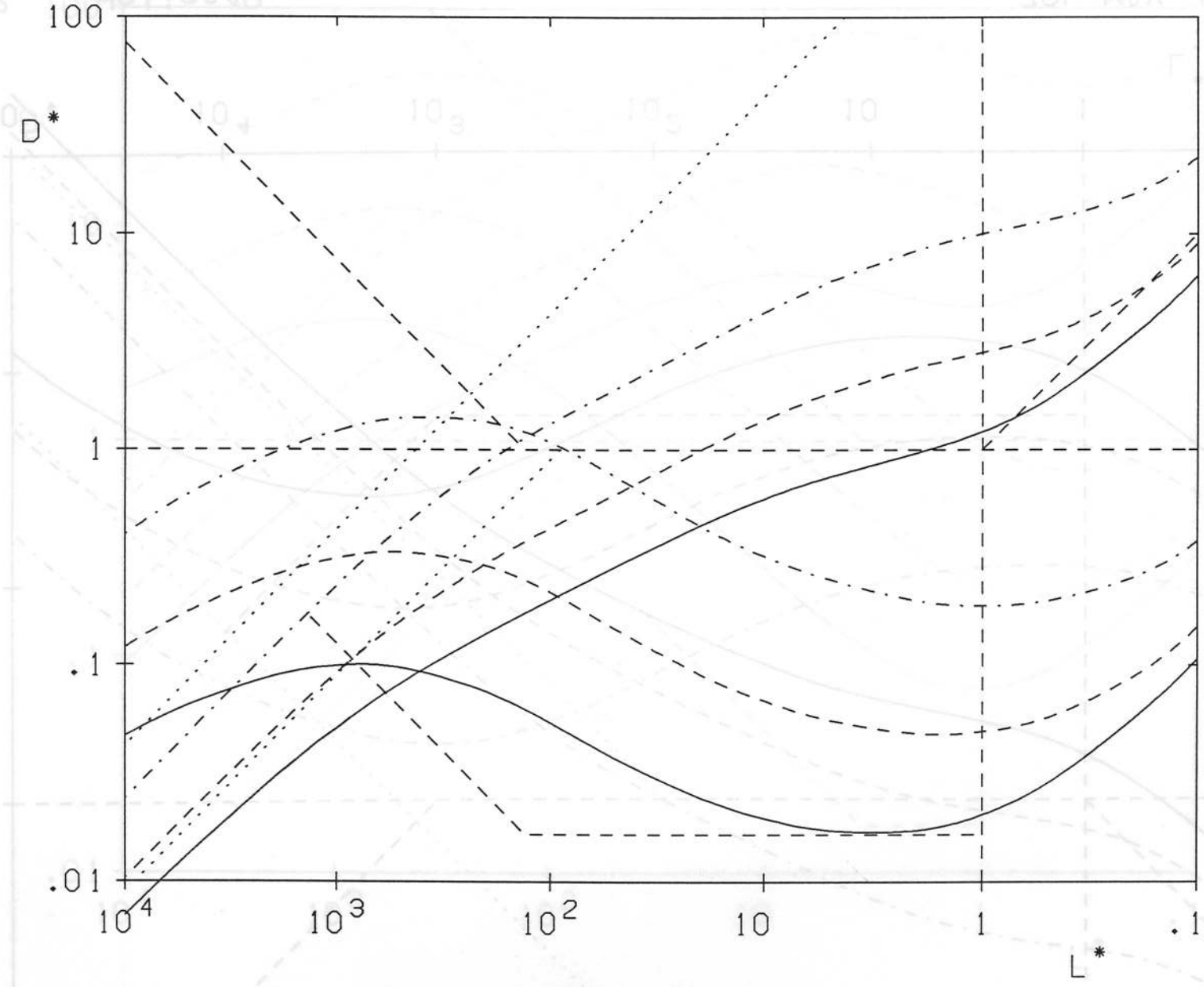

FIG. 11 Stellarator W VII-AS

ZOL:MAX.JW7AS

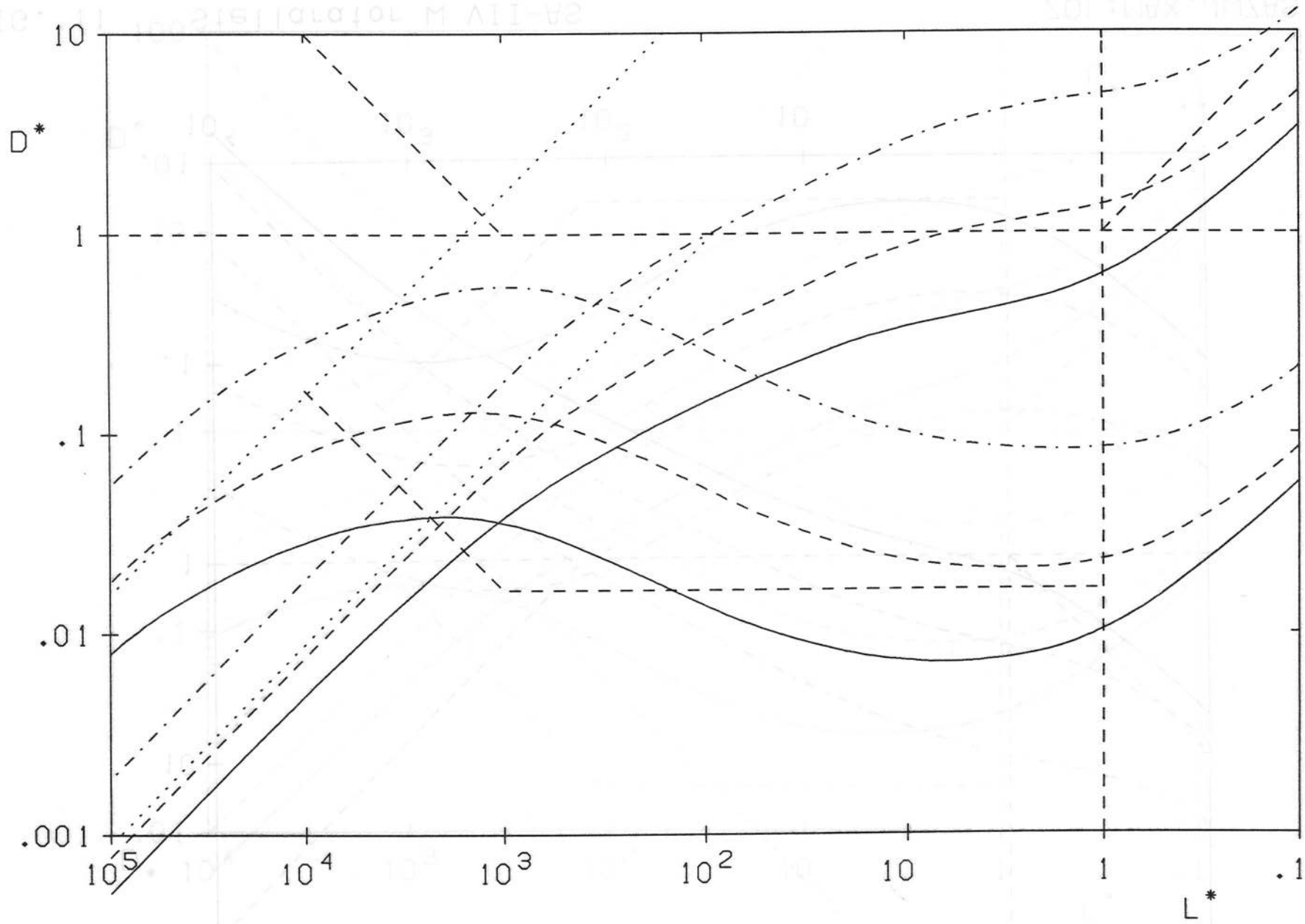

FIG. 12 Helias49

ZOL:MAX.JHEL49

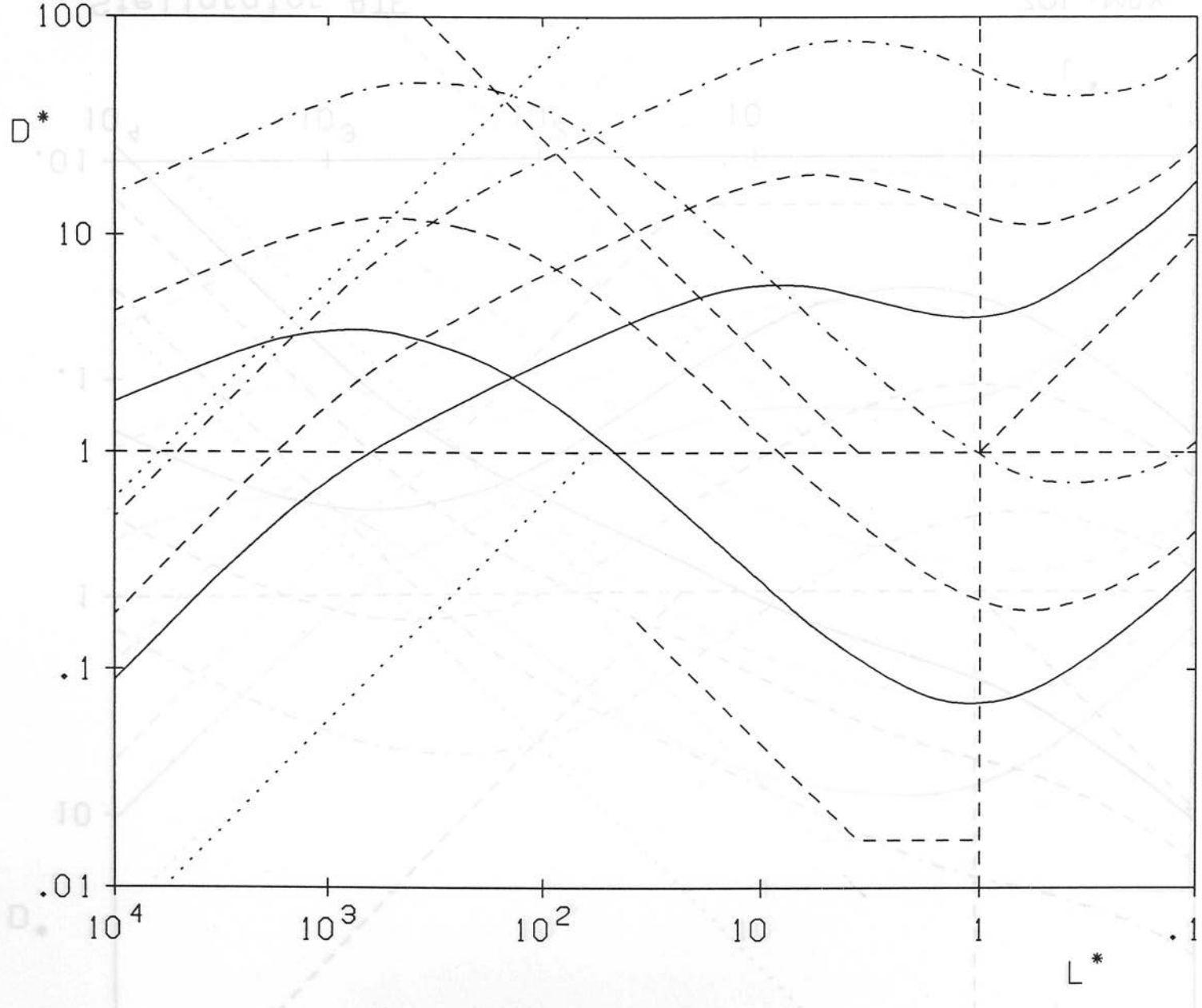

FIG. 13 Stellarator TJ-II

ZOL:MAX.JTJ2

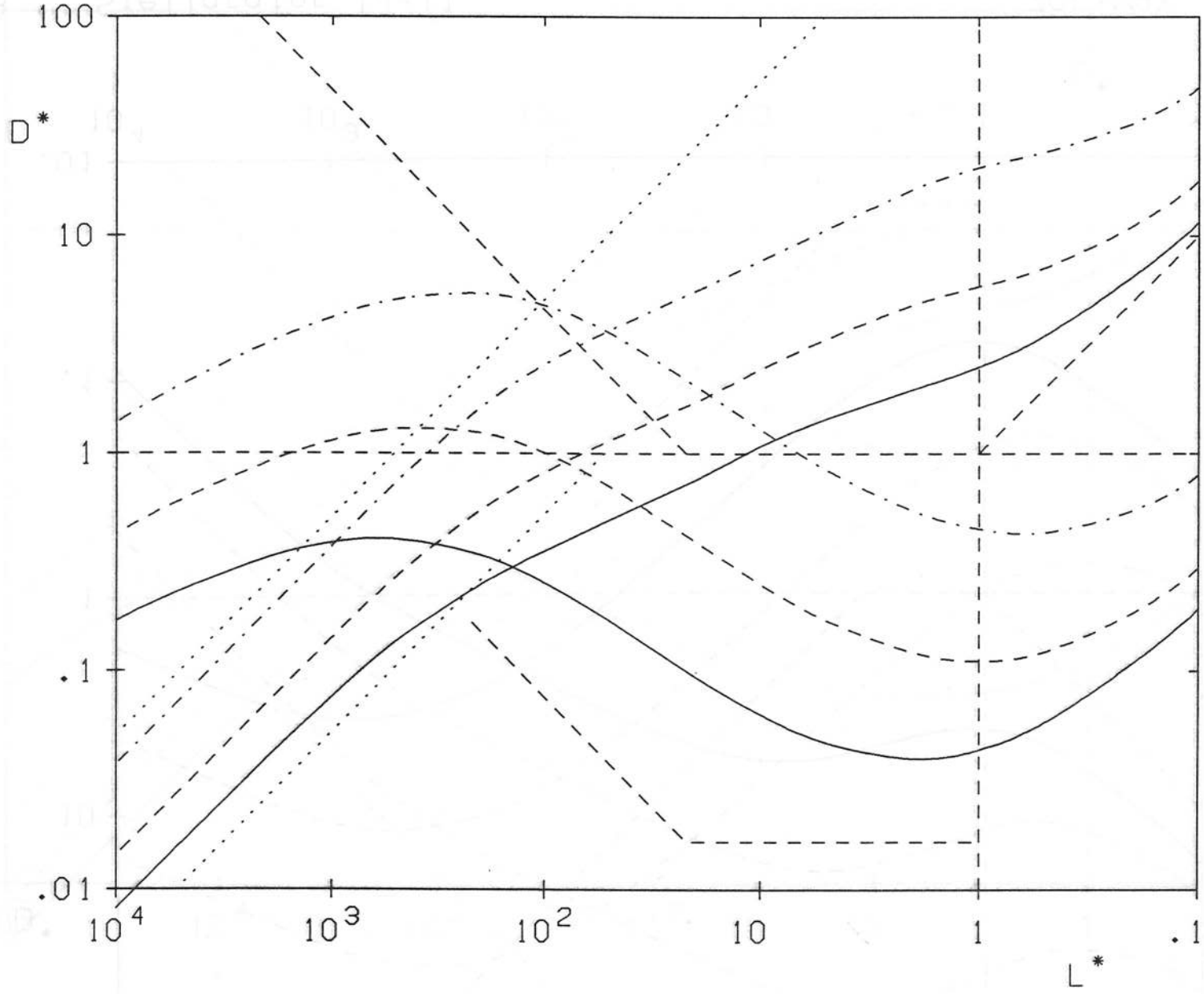

FIG. 14 Stellarator ATF

ZOL:MAX.J14ATF

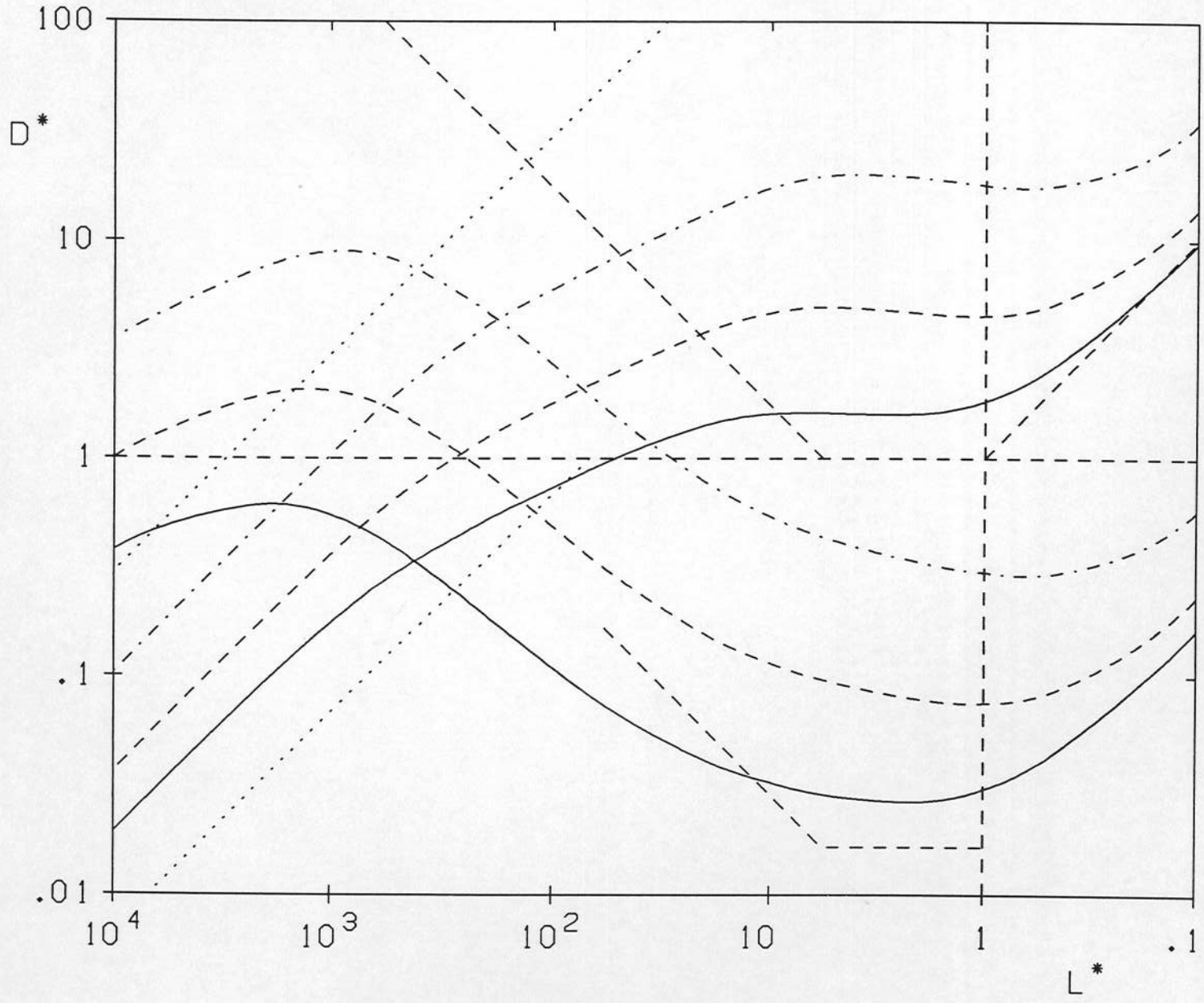

FIG. 15 Heliotron

ZOL:MAX.J17HELI